Title

Prolonged smoldering Douglas fir smoke inhalation augments respiratory resistances, stiffens the aorta, and curbs ejection fraction in hypercholesterolemic mice.

Authors

Eden, Matthew

Matz, Jacqueline

Garg, Priya

et al.

Publication Date

2023-02-25

DOI

10.1016/j.scitotenv.2022.160609

HHS Public Access

Author manuscript

Sci Total Environ. Author manuscript; available in PMC 2023 December 06.

Published in final edited form as:

Sci Total Environ. 2023 February 25; 861: 160609. doi:10.1016/j.scitotenv.2022.160609.

Prolonged Smoldering Douglas Fir Smoke Inhalation Augments Respiratory Resistances, Stiffens the Aorta, and Curbs Ejection Fraction in Hypercholesterolemic Mice

Matthew J. Eden, BS[A,*], **Jacqueline Matz, BS**[A,*], **Priya Garg, MS**[B], **Mireia Perera Gonzalez, BS**[A], **Katherine McElderry**[A], **Siyan Wang, BS**[B], **Michael J. Gollner, PhD**[B], **Jessica M. Oakes, PhD**[A,†], **Chiara Bellini, PhD**[A,†]

[A]Department of Bioengineering, Northeastern University, MA, USA.

[B]Department of Mechanical Engineering, University of California, Berkeley, CA, USA

Abstract

While mounting evidence suggests that wildland fire smoke (WFS) inhalation may increase the burden of cardiopulmonary disease, the occupational risk of repeated exposure during wildland firefighting remains unknown. To address this concern, we evaluated the cardiopulmonary function in mice following a cumulative exposure to lab-scale WFS equivalent to a mid-length wildland firefighter (WLFF) career. Dosimetry analysis indicated that 80 exposure hours at a particulate concentration of 22 mg/m^3 yields in mice the same cumulative deposited mass per unit of lung surface area as 3,600 hours of wildland firefighting. To satisfy this condition, male Apoe$^{-/-}$ mice were whole-body exposed to either air or smoldering Douglas fir smoke (DFS) for 2 hrs/day, 5 days/week, over 8 consecutive weeks. Particulate size in DFS fell within the respirable range for both mice and humans, with a count median diameter of 110±20 nm. Expiratory breath hold in mice exposed to DFS significantly reduced their minute volume (DFS: 27±4; Air: 122±8 mL/min). By the end of the exposure time frame, mice in the DFS group exhibited a thicker (DFS: 109±3; Air: 98±3 μm) and stiffer (DFS: 23±1; Air: 28±1 MPa^{-1}) aorta with reduced diastolic blood augmentation capacity (DFS: 53±2; Air: 63±2 kPa). Cardiac magnetic resonance imaging further revealed larger end-systolic volume (DFS: 14.6±1.1; Air: 9.9±0.9 μL) and reduced ejection-fraction (DFS: 64.7±1.0; Air: 75.3±0.9 %) in mice exposed to DFS. Consistent with increased airway epithelium thickness (DFS: 10.4±0.8; Air: 7.6±0.3 μm), airway Newtonian resistance was larger following DFS exposure (DFS: 0.23±0.03; Air: 0.20±0.03 cmH_2O-s/mL). Furthermore, parenchyma mean linear intercept (DFS: 36.3±0.8; Air: 33.3±0.8 μm) and tissue

Address for correspondence: Chiara Bellini, PhD, Department of Bioengineering, Northeastern University, 360 Huntington Ave. Boston MA 02115, c.bellini@northeastern.edu, Phone: (617) 373 2550.

*Authors contributed equally

†Authors contributed equally

CONTRIBUTIONS

CB and JMO conceptually developed and supervised all aspects of the project. PG and MJG designed the smoke generation apparatus and characterized the gaseous and particulate species, assisted by SW. MJE and JM designed the exposure circuit and chamber. MJE characterized the smoke, collected plethysmography data, and performed dosimetry modeling. KE performed daily mouse exposures. JM measured COHb and performed endpoint biomechanical assessments of the vascular and respiratory systems. MPG acquired endpoint cardiac MR images. MJE, JM, MPG, JMO, and CB analyzed and interpreted the data. MJE, JM, MPG, JMO, and CB drafted the manuscript and all authors reviewed it.

COMPETING INTERESTS

Nothing to declare.

thickness (DFS: 10.1±0.5; Air: 7.4±0.7 μm) were larger in DFS mice compared to air controls. Collectively, mice exposed to DFS manifested early signs of cardiopulmonary dysfunction aligned with self-reported events in mid-career WLFFs.

Keywords

Wildland fire smoke; Particulate matter; Dosimetry; Carboxyhemoglobin; Aortic distensibility; Airway morphometry

1. INTRODUCTION

The extent, severity, and frequency of wildland fires have worsened in recent years[1] due to the warming climate, growing population, enlargement of the wildland-urban interface, and progressive buildup of organic material and debris in regions of frequent fire suppression.[2,3,4] Historical data from the U.S. Environmental Protection Agency indicate that approximately one-third of carbon monoxide (CO), volatile organic compounds (VOCs), and respirable particulate matter ($PM_{2.5}$) in air originates from wildland fire smoke (WFS).[5] Epidemiological evidence shows that the release of $PM_{2.5}$ from WFS escalates the immediate risk of all-cause, respiratory, and cardiovascular mortality,[6,7,8,9] while brief exposure to WFS increases the rate of ambulance dispatches,[10,11] emergency room visits,[12,13,14,15] and hospital admissions[16,17] for cardiopulmonary complications. Complementary to these findings, rodent models of short-term exposure to lab-scale WFS have been instrumental in characterizing the biological responses that promote acute cardiovascular and respiratory events, as a function of different fuel sources, combustion conditions, PM concentrations, and inhalation patterns.[18,19,20,21,22,23] Although it is reasonable to expect that the accumulation of these insults over time may cause permanent damage to cardiopulmonary tissues and organs, the health outcomes of prolonged WFS inhalation remain unclear.

This lack of information poses a particular concern for wildland firefighters (WLFFs), whom repeatedly experience high-intensity exposures because of their proximity to the fire both during active duties and when resting at camp. Although WLFFs inhale large amounts of smoke as a result of increased respiratory and ventilation parameters under intense physical activity,[24] they rarely deploy respirators or other respiratory personal protective equipment due to extreme heat and lengthy work hours. The seasonal nature of employment and the cross-seasonal mobility of workers pose an obstacle to performing longitudinal studies in WLFFs.[25] As a result, little evidence is currently available to prospective recruits regarding the long-term occupational risks of wildland firefighting.[4,26]

Decline in lung function, respiratory symptoms, airway and systemic inflammation, and systemic arterial stiffening have been documented in WLFFs across a single work-shift or season (cf. Naeher et al.[27] and Adetona et al.[26] for thorough reviews). A recent study has further shown a cross-seasonal increase of total and LDL cholesterol levels in the blood of WLFFs, indicative of worsening metabolic and cardiovascular health.[28] The only investigation to date on the long-term health hazards of wildland firefighting reveals a significant positive association between years of service and self-reported prevalence

of hypertension and arrhythmia, with a similar trend for hypercholesterolemia.[29] To compensate for the lack of epidemiological evidence, a limited set of chronic lab-scale WFS exposures have been performed in rodents for up to 7 months.[30,31,32,33] These studies often take advantage of dosimetry modeling[34,35,36] to determine the (equivalent) concentrations of PM that either humans or rodents need to inhale in order to experience the same deposited PM mass per unit of lung surface area, should they endure the same amount of exposure days.[32] However, given the short lifespan of rodents, this method does not lend itself to studies long enough to be considered chronic for humans. Furthermore, rodents and humans age at a different pace, therefore typical exposure patterns in WLFFs cannot be easily replicated in animal studies. Hence, there is a need to develop novel methods to establish equivalent exposure conditions across species, such that the health effects associated with multiple years of wildland firefighting may be inferred from periods of exposure that are compatible with the mouse lifespan.

In an effort to investigate the cardiopulmonary outcomes of a mid-length WLFF career, we propose here an alternative approach, whereby we determine the combination of exposure duration and average PM concentration for our mouse exposures that yields the same deposited PM mass (normalized to the lung surface area) as 3,600 cumulative hours of WLFF service, while maintaining the concentration of CO below acutely toxic levels. Collectively, our findings indicate that mice manifest signs of cardiopulmonary dysfunction when exposed to smoldering Douglas fir smoke (DFS) for time and concentration conditions equivalent to an average mid-career WLFF.

2. MATERIALS AND METHODS

2.1. Exposure system for generation of smoldering DFS

We designed a custom exposure system inspired by DIN 53436[37,38] to produce, dilute, and distribute smoldering DFS to mice (Fig. 1, A). We sourced branches of Douglas fir (DF) trees from Missoula (MT), due to their prevalence in fire-prone ecosystems, availability, and ease of storage. Following separation from the branches, needles were dried in a 75 °C oven for 72 hours, then refrigerated until use. To generate the smoke,[39] needles were evenly distributed inside a quartz tube and combusted with a traveling ceramic heater mounted onto a linear actuator (Fig. 1, D). Temperature (450 °C), moving speed (20 mm/min), and primary air flow rate (3 L/min) were set to create smoldering combustion conditions.[39] The extent of dilution was chosen to reach target PM concentrations within the exposure chamber.

2.2. Chemical analysis of gases and particulates in DFS

Samples of DFS particulates were collected on quartz filters at the duct exhaust of the furnace (Fig. 1, A). The percentages of organic and inorganic (i.e., carbon black) material deposited on the quartz filters were determined with a thermo-gravimetric analyzer (model Discovery TGA 55; TA Instruments, New Castle, DE) under nitrogen and air atmospheres, respectively. VOCs trapped in the quartz filters were analyzed by heated headspace gas chromatography-mass spectrometry (HS GC–MS; model 6890A GC and model 5973 MS; Agilent Technologies, Palo Alto, CA).

The gaseous phase of DFS was sampled at the quartz tube outlet of the furnace (Fig. 1, A) with a heated probe. Sampling conditions were maintained at 650 torr and 100°C to avoid gas condensation. Real-time concentrations of target gases were measured by Fourier-transform infrared (FTIR) spectroscopy (model Nicolet iG50; Thermo Scientific, Franklin, MA).

Additional details on the methods for the chemical profiling of gases and particulates in DFS are reported in the Supplementary Material.

2.3. Morphometric analysis of particulates in DFS

We reconstructed the size distribution (by count) of particles in DFS by combining measurements from an Engine Exhaust Particle Sizer (EEPS model 3090; TSI, Shoreview, MN) and an Optical Particle Sizer (OPS model 3330; TSI, Shoreview, MN) that collectively span a 5.6 nm to 10 μm size range, as previously described.[40,41] The mean and dispersion of the particle size distribution were characterized by calculating the count median diameter (CMD) and the geometric standard deviation (GSD), respectively.

We visualized the shape of the particulates in DFS using Transmission Electron Microscopy (TEM; JEM-1010; JEOL, Tokyo, Japan). Particles were collected onto 300 mesh copper grids covered with a pure carbon support film (Ted Pella, Inc., Redding, CA). To improve particle adhesion, grids were dipped in a droplet of alcian blue for 5 minutes, then rinsed with deionized water and dried prior to placement just upstream of the whole-body exposure chamber, where smoke was delivered continuously for 30 minutes. Particles that adhered to the grids were negatively stained with uranyl acetate to improve contrast for image acquisition. Three non-overlapping regions from two grids were imaged at 2000x magnification (N = 6 images total). The particle analysis tool[42] in ImageJ (NIH, Bethesda, MD) was used to isolate DFS particulates and calculate their circularity as $\phi_{circ} = 4\pi A_p / P_p^2$, where A_p is the particle area and P_p is the particle perimeter. A circularity of $\phi_{circ} = 1$ describes a perfect circle, whereas $\phi_{circ} \to 0$ reflects a shape with finite area but infinite perimeter.

2.4. Animals

All experiments involving animals received approval from the Northeastern University Institutional Animal Care and Use Committee (IACUC) and complied with National Institute of Health (NIH) guidelines. Male Apoe$^{-/-}$ mice on a C57BL/6 background were purchased from The Jackson Laboratory (Bar Harbor, ME) at 8-weeks of age. Exposure to particulate matter raises blood cholesterol levels in humans,[43,44] thereby providing a substrate for the oxidative damage that often contributes to the adverse health outcomes of environmental air pollution inhalation. Unlike wildtype mice that maintain low blood cholesterol levels even when exposed to cigarette smoke,[45] Apoe$^{-/-}$ mice naturally exhibit elevated lipid and cholesterol profiles.[46,47] On account of this feature, we showed that Apoe$^{-/-}$ mice chronically exposed to cigarette smoke experience the same cardiovascular and respiratory ailments of habitual smokers.[48,49] These findings motivated the use of Apoe$^{-/-}$ mice as a preclinical model to study the cardiopulmonary occupational risk associated with WFS inhalation. All mice were housed in groups of up to 5 on a 12-hr

light/dark cycle under controlled temperature and with *ad libitum* access to standard chow and water.

2.5. Whole-body exposure chamber for the uniform delivery of DFS

Mice inhaled DFS while housed in a custom whole-body exposure chamber 3D-printed in ABS plastic (Stratasys F170 FDM 3D Printer; Stratasys, Rehovot, Israel). We iterated on the design of the chamber based on predictions of computational fluid dynamics simulations (Fig. 1, C; details in Supplementary Material) to attain uniform distribution of the smoke throughout.[50] Key design features include a cylindrical base 42 cm in diameter, a dome shaped top, a disk below the inlet to disperse the smoke, perforated floor and dividers, four outlet pipes underneath the floor, and 8 symmetrical compartments each holding up to 5 mice, thus enabling the concurrent exposure of up to 40 mice (Fig. 1, B). Inlet and outlet flow rates were set to 5 L/min to allow >15 air changes per hour.[51] Uniformity of PM concentration across the chamber was gravimetrically confirmed with 47-mm glass filter cassettes (Advantec®, Dublin, CA) positioned in each compartment and sampled at a flow rate of 5 L/min (GilAir Plus, St. Petersburg, FL).

2.6. Quantification of carboxyhemoglobin in the mouse blood

Noting that particulate inhalation greatly contributes to WFS toxicity,[19,23,18] we aimed to maximize the PM concentration in the smoke, while maintaining blood carboxyhemoglobin (COHb) levels below the ~15% threshold for CO injury in mice.[52] To probe the relationship between fuel mass, smoke PM and CO concentrations, and blood COHb levels, DFS generated from the combustion of either 1.5g, 2.25g, 3.75g, or 5.75g needle mass was delivered to mice (N = 5 per group) under the same dilution conditions. Mice were exposed for two consecutive 1-hr periods, separated by a brief refueling window. PM concentration was continuously monitored with a MicroDust Pro (Casella, Bedford, UK) calibrated with 47-mm glass fiber filters. CO, carbon dioxide (CO_2), and oxygen (O_2) levels in the chamber were concurrently recorded with an Enerac 700 (Enerac, Holbrook, NY). Blood was collected from anesthetized mice (2% isoflurane) via submandibular bleed immediately after the end of the second exposure period. Blood COHb levels were measured with an ABL80 CO-OX OSM (Radiometer America, Brea, CA). Linear regression analysis was used to estimate coefficients of proportionality and offsets between variables.

2.7. Monitoring of breathing waveforms during exposure

We recorded respiration waveforms using whole-body barometric plethysmography (N = 5 DFS, N = 5 Air), following protocols detailed elsewhere[41] and summarized in the Supplementary Material. Volume traces were calculated from pressure data[53] to extract respiratory rate (RR), inspiration time (t_I), first and second (when present) expiration times (t_{E1},t_{E2}), braking or breath hold time (t_H; Fig. 2, J), and tidal volume (TV), with minute volume determined as $MV = TV \cdot RR$. These parameters further facilitated calculation of representative volume curves for the two exposure groups.[41]

2.8. Dosimetry modeling to establish equivalent exposure conditions

Because of differences in the aging rate between humans and mice, we chose not to incorporate episodic exposure patterns in our study. Rather, we postulated that equivalent exposure conditions may be determined across species by matching the cumulative PM mass that deposits within the lower respiratory tract (LRT), normalized by the combined surface area of the tracheobronchial and respiratory zones.

We estimated the cumulative deposited mass as $m_{dep} = \dot{m}_{dep} \cdot t_h$, where $\dot{m}_{dep}$ is the mass deposited per hour of exposure and t_h is the total number of exposure hours. We assumed that mice experienced the same amount of deposited mass during each exposure, such that

$$\dot{m}_{dep,M} = \bar{C}_M \cdot MV_M \cdot dep_{f,M}, \quad (1)$$

where $\bar{C}_M$ is the average PM concentration of DFS within the exposure chamber, MV_M is the minute volume from plethysmography data, and $dep_{f,M}$ is the deposition fraction in the LRT, with subscript M for mouse. We considered a single work shift as the reference exposure instance for WLFFs. Assuming the same average shift duration throughout the cumulative exposure, we derived (see Supplementary Material) a weighted expression for the deposited mass per shift hour as

$$\dot{m}_{dep,W} = \sum_j \bar{C}_W \cdot MV_W{}^j \cdot dep_{f,W}{}^j \cdot f_s{}^j, \quad (2)$$

where $\bar{C}_M$ is the average PM concentration of WFS, $MV_W{}^j$ is the minute volume pertaining to shift segment j, $dep_{f,W}{}^j$ is the deposition fraction in the LRT for shift segment j, and f_s^j is the duration of shift segment j expressed as a fraction of the average shift duration, with subscript W for WLFF. We partitioned a typical shift by activity level (Table 1), whereby each segment accounts for the fraction of the shift when WLFFs exhibit heart rate (HR) within a set range.[24] We calculated corresponding ventilation parameters based on the exponential relationship between HR and MV.[54] Note, we used a representative heart rate of 90 beats/min for the lowest activity level and incremented by 20 beats/min thereafter.

We employed a custom 1D single-path dosimetry model (see Supplementary Material) to predict deposited mass fractions in the LRT of mice ($dep_{f,M}$) and WLFFs ($dep_{f,W}{}^j$).[55] Dosimetry calculations swept the range of particle sizes in DFS (Fig. 2, D) and treated particles as non-interacting, spherical, and with the typical density of burning biomass (ρ_p = 1.18 g/mL).[56] We assumed a sinusoidal respiratory flow rate for WLFFs and leveraged nomograms by Naranjo et al.[57] to estimate RR^j and TV^j for each MV^j instance throughout a shift. Note, we followed a “normal augmenters” definition for the distribution of oronasal respiratory airflow in WLFFs.[58] We further determined the breathing flow rate in mice by taking the time derivative of the average experimental lung volume curves[59] (Fig. 2, H and J). Functional residual capacity (FRC) was set to 0.6 mL for mice[35] and 3000 mL for WLFFs.[60]

2.9. Estimating the cumulative duration of mouse exposure

Parameters involved in the equivalent exposure analysis are listed in Table 2. We targeted $t_{h,W}$ = 3,600 exposure hours to represent a mid-length WLFF career that lasts from 3 to 7 years and may include between 49 and 98 shifts per year,[25] with shift duration ranging from 10.3 to 13.6 hours,[61,25] at an average PM concentration of 0.51 mg/m^3 throughout.[25] Leveraging Equations 1 and 2, we solved for the cumulative hours that support an equivalent exposure in mice

$$t_{h,M} = \frac{\dot{m}_{dep,W} \cdot t_{h,W}}{SA_W} \cdot \frac{SA_M}{\dot{m}_{dep,M}}, \quad (3)$$

where SA_W = 67.5 m^2 is the lung surface area in WLFFs[60] and SA_M = 0.0454 m^2 is the lung surface area in mice.[35] As rationalized in Sections 3.1, 3.2, and 3.6, we attained the desired $t_{h,M}$ by exposing mice (N = 27) to smoldering DFS at a target concentration of 22 mg/m^3 for 2 hours/day, 5 days/week, for 8 consecutive weeks. Age-matched mice (N = 27) exposed to HEPA-filtered air acted as controls. PM and CO concentrations in the chamber were measured during each exposure using gravimetric analysis and the Enerac 700, respectively.

2.10. Longitudinal monitoring of physiological parameters

Body mass (all animals), resting peripheral blood pressure (N = 8 DFS, N = 8 Air), and blood COHb (N = 18–20 DFS, N = 12–16 Air) were measured once a week throughout the study. A noninvasive tail-cuff system (CODA; Kent Scientific, Torrington, CT) facilitated collection of pressure tracings in awake but restrained mice, with baseline acclimation to mitigate stress-related artifacts. Blood was drawn immediately after exposure to determine COHb levels as described in Section 2.6. At the end of the 8-week time frame, and at least 24 hours after the last exposure, mice underwent either *in vivo* assessment of respiratory and cardiac function, or their aorta was excised for *in vitro* mechanical testing.

2.11. Assessment of aortic function by biaxial testing

Anesthetized (2% isoflurane) mice (N = 9 DFS, N = 10 Air) were sacrificed via cervical dislocation to harvest the abdominal aorta for mechanical characterization, according to experimental protocols and analytical methods described elsewhere[49] and summarized in the Supplementary Material. Parameters of a microstructurally motivated four-fiber family strain energy potential were estimated from experimental data and used to predict geometry and tissue properties under physiological loads. The small-on-large approach allowed for calculation of biaxial linearized stiffness about the desired working point.[62] Cyclic structural stiffness was further evaluated in terms of aortic distensibility

$$\mathscr{D} = \frac{d_{sys} - d_{dias}}{d_{dias} \cdot (P_{sys} - P_{dias})}, \quad (4)$$

where P and d refer to luminal pressure and diameter, respectively, with subscript *dias* for diastole and *sys* for systole.

2.12. Visualization of aortic wall microstructure

Following functional testing, abdominal aortic samples were processed for histology, according to the methods reported in the Supplementary Material. Aortic cross-sections were stained with Movat's pentachrome and Picrosirius red stains.

2.13. Assessment of cardiac function by magnetic resonance imaging

Cardiac magnetic resonance (MR) imaging was performed with a 7.0-T BioSpec MR system (Bruker Biospin MRI, Billerica, MA) under ECG and respiratory gating (SA instruments, Stony Brook, NY). Mice (N = 9 DFS, N = 8 Air) were anesthetized with isoflurane (4% induction, 1–2% maintenance) and positioned prone on a mouse cradle. A total of 6 to 9 short-axis cine gradient-echo fast low angle shot images were acquired to encompass the entire volume of the left ventricle. Sequence parameters were: 30° flip angle; 6 ms repetition time; 1.85 ms echo time; 0.2 × 0.2 mm matrix spatial resolution; 4 signal averages. Anesthetized mice were sacrificed by cervical dislocation following MR imaging. Endocardial and epicardial regions of the left ventricle were manually delineated with the software Segment Medviso[63] (Fig. 3, H) and used to determine end-diastolic (EDV) and end-systolic (ESV) volumes for calculation of the ejection fraction

$$EF\% = \frac{EDV - ESV}{EDV} \cdot 100. \tag{5}$$

2.14. Assessment of respiratory function by mechanical ventilation

Respiratory function was measured in anesthetized mice (N = 9 DFS, N = 9 Air) using standard forced oscillatory techniques[64] at a positive end expiratory pressure P_{peep} = 1 cmH_2O, as detailed in the Supplementary Material. Anesthetized mice were sacrificed by exsanguination following mechanical ventilation. Respiratory system resistance (R_{rs}) and reactance (X_{rs}) were determined by taking the real and imaginary part of the lung impedance (Z), respectively. Airway (Newtonian) resistance (R_N), coefficient of tissue elastance (H), and coefficient of tissue resistance (G) were estimated from impedance data by fitting the constant phase model[65]

$$Z(\omega) = R_N + \frac{(\eta - j)H}{\omega_n^{\alpha}}, \tag{6}$$

where ω_n is the angular frequency normalized by 1 rad/s,[66] j is the imaginary unit, and $\eta = G/H$ is the hysteresivity, which is also necessary to calculate $\alpha = \frac{2}{\pi} tan^{-1}\left(\frac{1}{\eta}\right)$.

2.15. Evaluation of airway morphometry

Upon completion of functional testing, lungs were processed for assessment of airway morphometry (N = 4 DFS, N = 4 Air), following methods reported in the Supplementary Material. Mean linear intercept (L_m), bronchi thickness, and parenchyma tissue thickness were quantified from images of Movat's pentrachrome-stained tissues. Measurements were performed in three separate regions from the apical, middle, and base sections of the left and apical lobes. As the airway thickness depends on surrounding tissues, we limited

our analysis to the epithelium, calculating the average distance between two segmented contours. Sections of parenchyma used for thickness and airspace measurements did not include airways or blood vessels.

2.16. Statistical analysis

Unless specified, data is presented as mean ± SEM. Goodness of fit was expressed in terms of R^2 for linear regressions, $RMSE$ (root mean square error) for nonlinear regressions of aortic mechanics data and χ^2 (Pearson's Chi Square Test) for the fitting of lung impedance data. Student's t test was used to analyze the influence of DFS exposure on ventilation parameters, longitudinal physiological data, metrics describing the structure and function of the aorta, left ventricular volumes and ejection fraction, and structural and functional parameters of the respiratory system. Statistically significant difference was set to $p < 0.05$.

3. RESULTS

3.1. A custom system facilitates the exposure of mice to DFS

Performances of both the smoke-generating equipment and the exposure chamber constrained the number of daily exposure hours that counted toward the desired cumulative exposure time (i.e., $t_{h,M}$ in Equation 3). Computational fluid dynamics simulations showed a uniform normalized particle concentration in the exposure chamber (Fig. 1, C) and average filter mass varied by <10% from the mean concentration across all compartments (Table S1). Combined, these outcomes confirmed that mice experienced similar exposure conditions regardless of their placement within any of the chamber compartments.

The ceramic quartz-tube furnace[39] initiated smoldering combustion of dried DF needles while it travelled along the boat (Fig. 1, D). Gaseous and particulate emissions delivered to the exposure chamber exhibited a rapid increase at first, then stabilized for ~1 hour before refueling was necessary (Fig. 1, E for a 3.75 g fuel load). Brief spikes in CO and PM concentrations that occurred throughout each hour-long installment either marked the initial combustion of DF needles as the ceramic heater moved over them or reflected minor heterogeneity in fuel distribution along the boat.

Overall, accounting for preparation and clean-up time, we concluded that it was feasible to simultaneously expose up to 5 mice per compartment, or 40 mice total, for 2 hours/day.

3.2. A 3.75 g target fuel mass maximizes PM concentration while avoiding CO-induced injury in mice

Preserved combustion parameters and dilution factors[40] upheld a linear relationship between the concentration of both PM (Fig. 2, A) and CO (Fig. 2, B) in the smoke and the mass of dried DF needles loaded onto the quartz boat. COHb levels in the mouse blood were also linearly related to fuel mass (Fig. 2, C), confirming that smoke CO concentrations up to ~200 ppm did not saturate hemoglobin in the mouse blood nor caused acute toxicity (COHb >50% in the mouse[52]). Empirical correlations between system input, aerosol properties, and exposure biomarker (regression lines in Fig. 2, A–C) facilitated solving for the amount of fuel that could maximize the smoke PM concentration without exceeding the threshold for

CO-induced injury (COHb >15% in mice[52]). Motivated by the confidence intervals on the regression parameters (shaded areas in Fig. 2, A–C), we selected 3.75 g as the target fuel mass for our long-term exposure study, expected to yield 11.3% COHb in the mouse blood while supplying 22 mg/m^3 PM and 139 ppm CO concentrations in the smoke.

3.3. Gaseous and particulate fractions in DFS contain harmful chemicals

Particulates in DFS were entirely composed of organic material that volatilized within the inert TGA atmosphere. The absence of black carbon, which forms at high temperature under flaming conditions,[39] aligns with a modified combustion efficiency index *MCE* = 80.37 that nears the threshold for pure smoldering combustion.[67] Note, Jen et al. also found that black carbon remained at background levels in smoldering Douglas fir litter smoke with a similar MCE.[68]

Concentrations of VOCs in smoldering DFS particulates as resolved by GC–MS are reported in the Supplementary Material (Table S2). Polyols and phenols similar to 2-O-Methylhexose ($C_7H_{14}O_6$), D-Allose ($C_6H_{12}O_6$), and m-Carbomethoxyphenol ($C_8H_8O_3$) were the most abundant and accounted for ~15% of the total volatile concentration.

Levels of target gaseous species in smoldering DFS remained relatively stable over the FTIR acquisition window (data not shown), serving as an additional indication that our exposure system (Fig. 1, A) was able to produce consistent emissions. Average concentrations for the top 15 of the target gases are listed in the Supplementary Material (Table S3). As expected, CO and CO_2 were the dominant gaseous effluents in smoldering DFS. Detection of unburned hydrocarbons, including methane (CH_4), butane (C_4H_{10}), and ethane (C_2H_6), as well as alcohols such as methanol (CH_3OH) confirmed that incomplete combustion occurred under smoldering conditions.

3.4. DFS particulates are within the respirable range for mice and humans

The size distribution of particulates in smoldering DFS was unimodal by count (Fig. 2, D), with an average (± 95% confidence interval, over three runs) CMD = 110 ± 20 nm and GSD = 1.47 ± 0.03. The lognormal probability distribution function using CMD and GSD as estimates of mean and variance well enveloped the experimental data (shaded area).

Particulates in DFS formed agglomerates with a varying number of primary units (Fig. 2, E) and were surrounded by an oily halo, as noted previously.[69] Over half of the particulates exhibited a circular shape with circularity score greater than 0.7, though longer chains of agglomerates with lower values of circularity were also noted (Fig. 2, F).

3.5. Mouse experience expiratory braking during DFS exposure

Pattern and frequency of breathing volumes determine the amount of inhaled mass and influenced the deposition of particles within the respiratory system, serving as necessary parameters for dosimetry modeling. When exposed to filtered air, mice exhibited expected periodic volume waveforms of rhythmic inhalation and exhalation (Fig. 2, G and H). Delivery of DFS altered the normal breathing pattern by introducing braking between two exhalation periods (Fig. 2, I and J). The dynamics of the expiratory flow, combined with

longer inhalation and exhalation times, reduced RR in mice exposed to smoke, compared to air controls (Table 3). As a result, the MV was also significantly diminished, despite no difference in TV (Table 3).

3.6. An 8-week long exposure paradigm in mice recapitulates a mid-length WLFF career

The fraction of inhaled mass that deposits in the LRT of WLFFs ranges from $dep_{f,W} = 0.321$ under resting conditions to ~0.350 at the highest activity levels (Table 1). However, given the distribution of physical effort throughout a typical shift, WLFFs experience the lowest mass deposition rate when their HR exceeds 180 beats/min, while the largest occurs within the 120–140 beats/min HR range (Table 1). Based on these predictions, the average mass deposition rate weighted by the relative duration of each shift segment equals $\dot{m}_{dep,W} = 0.42$ mg/hr. Therefore, throughout a mid-length career comprising 3,600 work hours, WLFFs cumulatively retain $m_{dep,W} = 1.5$ g PM mass, or 22.4 mg/m^2 when normalized by the lung surface area.

Noting that $dep_{f,M} = 0.354$ for mice, the mass deposition rate in their LRT amounted to $\dot{m}_{dep,M} = 0.0126$ mg/hr. As a result, ~80 hours of exposure to smoldering DFS at an average PM concentration of $\bar{C}_M = 22$ mg/m^3 was necessary to achieve the desired cumulative deposited mass per unit of lung surface area. To satisfy this requirement within the constraints of our exposure system, we set the duration of the study to 8 weeks, with mice exposed 5 days each week and 2 hours/day (Table 2).

3.7. Emissions remain stable throughout the 8-week exposure study

Throughout the course of the 8-week exposure, temperature and relative humidity within the exposure chamber averaged (± SD) 23.7 ± 1.1 °C and 42.8 ± 11.2 %, respectively. Smoke emissions remained close to target, with average (± SD) PM and CO concentrations of 22 ± 6 mg/m^3 and 125 ± 30 ppm, respectively. Consistently, weekly measurements of blood COHb levels exhibited little variation from the expected value, averaging at 11.1 ± 0.2% in mice exposed to smoldering DFS, compared to 2.0 ± 0.1% in air controls (Fig. S1, A). Collectively, these data confirm that mice experienced similar exposure conditions throughout the study. Furthermore, no acute lung injury due to CO inhalation should have occurred, given that the concentration of COHb in the mouse blood remained below the 15% threshold at all times.[52]

Average body mass continued to increase in all mice over the 8 weeks of exposure (Fig. S1, B, Supplementary Material). However, mice exposed to DFS gained weight at a slower pace and, by the end of the study, exhibited a significantly lower body mass compared to air controls.

3.8. Prolonged DFS exposure stiffens the aorta and reduces left ventricular ejection fraction

Peripheral blood pressure in air control mice remained close to baseline throughout the 8-week exposure time frame, with average systolic and diastolic values of 100 ± 1 mmHg and 71 ± 1 mmHg, respectively (Fig. 3, A). In contrast, exposure to DFS was associated with a linear increase in both systolic ($y = 0.55x + 101.58$, R^2=0.819,

p<0.001) and diastolic ($y = 0.62x + 73.20$, R^2=0.860, p<0.001) blood pressure (Fig. 3, A). Albeit subtle, augmented hemodynamic loads may promote or enhance changes in the compliance of the aorta that could propagate upstream to the heart and downstream to the microvasculature.[70] To substantiate this speculation, we performed mechanical tests on the abdominal aorta of mice exposed to either DFS or air. Consistent with our findings on the effect of cigarette smoking,[49] stress values within the expected *in vivo* range imposed larger circumferential deformations (Fig. 3, B) but smaller axial deformations (Fig. 3, C) in tissues from the aorta of mice in the DFS group, compared to air controls. While this contributed to maintaining circumferential tissue stiffness within physiological limits (Table S5, Supplementary Material), the decline in axial stretch (Fig. 3, D) reduced the elastic energy stored within the tissue at systole (Fig.3, E), thus impairing the ability of the aorta to augment diastolic blood flow. Furthermore, wall thickening (Fig. 3, F,L–N) enhanced the structural stiffening of the aorta, as indicated by decreased distensibility (Fig. 3, G). That is, although the tissue itself did not become stiffer, changes in the geometry of the aorta reduced the relative increase in the luminal diameter between diastole and systole. As a result, left ventricular ESV was significantly larger in mice that had been exposed to DFS for 8 weeks, compared to air controls (Fig. 3, J). Because no difference between groups was noted in left ventricular EDV (Fig. 3, I), ejection fraction was also reduced in DFS-exposed mice (Fig. 3, K). A summary of the best-fit model parameters (Table S4) and descriptors of material, geometrical, and structural metrics (Table S5) for the abdominal aorta are reported in the Supplementary Material. Measurements of cardiac volumes and ejection fraction are also provided in the Supplementary Material (Table S6).

3.9. Prolonged DFS exposure increases respiratory system and airway resistances

Respiratory system resistance R_{rs} at frequencies from 9.5 to 20.5 Hz was significantly larger in DFS-exposed mice compared to air controls (Fig. 4, A). No difference in respiratory reactance X_{rs} emerged between groups at any frequency (Fig. 4, B). Prolonged exposure to DFS was associated with significantly higher Newtonian resistance R_N (Fig. 4, C) and no change in the coefficient of tissue elastance H, the coefficient of tissue resistance G, and lung tissue hysteresivity η (Fig. 4, D–F) from air control. Morphological assessment showed airspace enlargement with increased L_m (Fig. 4, I–K) following DFS exposure. Thickening of airways primarily comprised of epithelial cells (Fig. 4, G–H,L) likely prompted the significant increase of R_N (Fig. 4, C). However, thickening of parenchyma septa (Fig. 4, M) did not alter H and G from air control levels (Fig.4, D–F). Best-fit constant phase model parameters are reported in the Supplementary Material (Table S7).

4. DISCUSSION

The relative contribution of wildland fire emissions to PM air pollution has increased by 10% over the past two decades,[5] due to longer wildfire seasons, more frequent wildfires, and larger burned areas.[1] The emergence of this trend triggered public health concerns, as PM remains the best predictor of the health risks associated with smoke exposure from most combustion sources.[27] In response, a growing body of literature has been exploring the association between an episodic rise in $PM_{2.5}$ from wildland fires and either mortality rates or health care facility traffic due to cardiovascular and respiratory

events within a few days of exposure (e.g. physician or emergency room visits, hospital admissions).[26,27,71] Notwithstanding these efforts, limited information exists on the burden of repeated smoke inhalation, including the occupational exposure inherent to wildland firefighting.[26,72,73] Since WLFFs experience harsher conditions compared to the general public, key stakeholders in the community strongly advocate for research to elucidate the long-term risks of non-accidental disease associated with wildland fire suppression.[74] As a complement to challenging epidemiological studies,[26] we inferred the health hazards of continued wildland firefighting from measurements of cardiopulmonary function in a mouse model of cardiovascular and respiratory comorbidity[46] following exposure to lab-scale DFS.[39] To establish equivalent exposure conditions, we leveraged dosimetry predictions and matched the PM mass that mice and WLFFs cumulatively retain, normalized by the surface area of the lungs in both species.[23,19,40] This approach provides a rationale for estimating, rather than arbitrarily choosing, the number of exposure hours in our preclinical model of smoke inhalation. Given the variability in shift and season duration, we expressed WLFF exposure in terms of cumulative work hours, which we anticipate could be exhausted over 3 to 7 years of service. Thus, our study offers unprecedented insights on the predicted burden of cardiopulmonary disease in the population of mid-career WLFFs.

4.1. Evidence of compromised cardiovascular function with repeated DFS inhalation

Since aortic stiffening is an independent risk factor for cardiovascular disease,[75] the significant lapse of aortic distensibility in mice exposed to DFS (Fig. 3, G) suggests that continued service across just a few fire seasons may jeopardize the cardiovascular health of WLFFs, as per the terms of equivalent exposure between mice and humans (Table 2). Our findings align with prior evidence of positive association between biomarkers of oxidative stress, biomarkers of WFS exposure, and measures of systemic arterial stiffness in WLFFs,[76] but provide further evidence on the key processes that mediate the cardiovascular outcomes of chronic WFS inhalation.

The concomitant occurrence of reduced distensibility (Fig. 3, G) and loss of energy storage (Fig. 3, E) shows that repeated DFS inhalation may undermine the fundamental role of the aorta as a pressure resevoir throughout the cardiac cycle. This significant deterioration of the Windkessel function has two profound implications for cardiovascular health.[70] First, it may damage the microvasculature due to the propagation of the pulsatile pressure wave toward peripheral tissues. Second, it heightens the risk of cardiac failure and ischaemia by increasing left ventricular workload and myocardial blood demand. Consistent with the latter, the volume of blood that remained in the left ventricle following cardiac systole was larger (Fig. 3, J) and caused a ~10% reduction of the ejection fraction (Fig. 3, K) in DFS-exposed mice. Since Martin et al. only noted a significant decrease of left ventricular EDV in rats exposed to flaming eucalyptus smoke for one hour (0.7 mg/m^3 PM concentration),[21] we presume that the effects of long-term DFS inhalation on left ventricular function observed here may be secondary to vascular adaptations and associated hemodynamics changes, rather than stem from repeated insults to the heart.

Pursuant to cross-sectional data showing that the odds of being diagnosed with hypertension and arrhythmia increase with the years of service in WLFFs,[29] systolic and diastolic values

of blood pressure in DFS-exposed mice at sacrifice exceeded baseline by 6% and 9%, respectively (Fig. 3, A). Interestingly, Martin et al. reported that blood pressure in rats rose up to ~10–15% above baseline throughout a sole hour of exposure to smoldering peat smoke at 4 mg/m^3 PM concentration, and remained elevated by less than 10% from baseline 3 hours post treatment.[20] In light of this evidence, our observations indicate that the transient intensification of hemodynamic loads upon WFS inhalation may lead to permanent alterations of cardiovascular function when sustained over time.

Superimposed to the modest increase in blood pressure, wall thickening (Fig. 3, F) largely contributed to the structural stiffening of the abdominal aorta in mice exposed to DFS (Fig. 3, G). Visual inspection of histological images suggests that DFS inhalation may widen the aortic wall by promoting collagen deposition in the adventitia (Fig. 3, L–N). We likewise reported that *de novo* collagen synthesis under gradually increasing pressure loads rendered the wall thicker while preserving intrinsic tissue properties in the abdominal aorta of Apoe$^{-/-}$ mice exposed to cigarette smoke.[49] Although we further showed that chronic cigarette smoking enhanced the vulnerability of spontaneous[46,47] atherosclerotic lesions at the root of the Apoe$^{-/-}$ mouse aorta,[49] neither exposure to cigarette smoke nor DFS promoted neointima formation in low-curvature segments such as the suprarenal abdominal aorta. Nevertheless, given that a single, one hour-long exposure to flaming eucalyptus smoke (0.7 mg/m^3 PM concentration) or smoldering peat smoke (0.4 mg/m^3 PM concentration) sensitized rats to the cardiovascular effects of high carbohydrate[21] or high fat[77] oral gavages, respectively, we anticipate that lifestyle choices may modulate both the functional and atherosclerotic burden of prolonged WFS inhalation, which should be addressed in future work.

4.2. Evidence of compromised respiratory health with repeated DFS inhalation

The enlargement of parenchyma airspaces (Fig. 4, K), the thickening of the airway epithelium (Fig. 4, L), and the increase in respiratory resistances (Fig. 4, A and C) detected in mice exposed to DFS are reminiscent of chronic obstructive pulmonary disease. From this evidence, we infer that the respiratory health of WLFFs may decline over a mid-length career due to the accumulation of adverse stimuli through repeated WFS inhalation, since spirometry parameters (e.g., forced expiratory volume in 1 second, maximum mid-expiratory flow, and forced vital capacity) deteriorate following a single wildland firefighting shift or season.[78,79,76] Consistent with this notion, epidemiological data show that respiratory function worsens with previous firefighting activity across multiple days and fire seasons.[80,78,81,82,83,84] Nevertheless, preclinical models of lab-scale WFS exposure as presented here remain crucial to fully characterize tissue- and organ-level responses that support observed functional shifts.

Compared to air-exposed mice, repeated inhalation of DFS led to a significant increase in R_N (Fig. 4, C) and R_{rs} at the higher frequencies (Fig. 4, A), with no observed differences in either G (Fig. 4, E) or low frequency R_{rs} (Fig. 4, A). Larger values of R_N and R_{rs} at the higher frequencies are indicative of central airway remodeling and suggest that mid-career WLFFs may experience difficulty breathing, perhaps in the form of enhanced airway hyper-responsiveness.[85] To substantiate the robustness of our approach, we note that

the average R_N for air-exposed male Apoe$^{-/-}$ mice at 16 weeks of age (Fig. 4, C) agrees with measurements reported elsewhere for 3- and 8-month-old naïve male Apoe$^{-/-}$ mice, respectively.[86] Akin to the larger R_{rs} of mice within our DFS group (Fig. 4, A), Tesfaigzi et al. found elevated total pulmonary resistance in rats exposed to pine wood smoke for up to 90 days at PM concentrations of 1 and 10 mg/m^3, with the former alone attaining a statistically significant difference from control.[30] However, the authors were unable to differentiate between changes in central versus peripheral resistances, since they did not perform a frequency sweep for R_{rs} nor reported changes in R_N.

Thickening of the bronchi due to epithelial cell hyperplasia (Fig. 4, G–H, L) is likely responsible for the increase of R_N (Fig. 4, C) in DFS-exposed mice, as noted by others in the context of fire smoke inhalation.[87,33,88] While not explored here, the transition of epithelial cells into a motile mesenchymal phenotype upon biofuel exposure[33] may complement the hyperplastic response.

Mice exposed to DFS further exhibited significantly larger L_m and thickening of parenchyma tissues compared to air controls (Fig. 4, K and M). However, these two structural adaptations likely compensated each other and did not lead to measurable differences in parenchyma function, i.e., the values of X_{rs} and H were comparable between the two groups (Fig. 4, B and D).

Aligned with our observations, but in guinea pigs, Ramos et al. reported a 1.05 fold increase of L_m above baseline in animals exposed to pine wood smoke for 2 months at ~0.4 mg/m^3 $PM_{2.5}$ concentration, which rapidly progressed to 1.96 and 2.91 after 4 and 7 months, respectively.[87] Destruction of lung parenchyma was associated with an early increase in BALF macrophage content and higher neutrophil counts at later time points, concomitant with enhanced MMP expression/activity and cell apoptosis, all of which play a role in the pathogenesis of emphysema.[87] Consistent with these findings, parenchyma tissues from rats exposed to smoldering China fir sawdust for 7 months featured a 60% larger L_m compared to controls, as well as enhanced alveolar septal cell apoptosis.[33] The degree of airspace destruction observed in both of these studies[33,87] was more pronounced than noted here, likely because of the longer exposure duration. However, neither of them addressed parenchyma tissue thickening nor associated functional changes of respiration. Future investigations are thus encouraged to evaluate the combined structural and functional remodeling of the parenchyma in the specific animal model of choice, as a function of fuel source, smoke concentration, and exposure duration.[33,30]

4.3. Breathing patterns during DFS exposure

Volume waveforms modulate the amount of inhaled mass that deposits within the respiratory tract[35] and are therefore instrumental in establishing the parameters for equivalent exposure between mice and WLFFs. Inhalation of DFS prompted immediate expiratory braking, shown as the flat portion of the representative volume curve (Fig. 2, J). The occurrence of a pause during expiration has been extensively described after administration of the sensory irritants[89] detected in DFS (Tables S2 and S3, Supplementary Material). Reflex glottis adduction upon stimulation of trigeminal nerve endings within the nasal mucosa may support, at least in part, these expiratory flow interruptions.[89,90] The associated

decline of *RR* and *MV* (Table 3) is consistent with prior observations in mice exposed to smoldering oak and eucalyptus smoke.[18] However, inhibition of respiratory movements may only be transient, since Kim et al. noted that ventilation volumes in mice were either preserved or elevated immediately after and 24 hours post exposure to peat, eucalyptus, and oak smoke, under flaming or smoldering combustion.[19] Nevertheless, incorporation of expiratory braking distinguishes our approach to dosimetry modeling and improves prediction of the mass that deposits in the respiratory system of smoke-exposed mice.

To circumvent the challenges of monitoring respiration in WLFFs while on duty, we leveraged predictive equations recently proposed by Cruz et al. to infer the *MV* based on *HR* under endurance exercise.[54] Because the physical demands of wildland firefighting vary widely throughout a shift,[24] our estimates ranged between 21 and 173 L/min for periods of low and high cardiovascular strain, respectively (Table 1). Weighted by the fraction of the shift pertaining to each activity level, these values converge to an average *MV* per shift of 41 L/min, in agreement with the 22 to 60 L/min range reported in previous studies.[25] Mirroring *MV*, the fraction of deposited mass along the respiratory tract varies from a minimum of 0.321 to a maximum of 0.350 within a shift (Table 1), further emphasizing the influence of breathing patterns and lung volumes on the deposited PM mass dose and the associated risk of developing adverse health effects.[25,91] Overall, accounting for within-shift effort fluctuations as we do here refines previous attempts to parallel exposure duration across species.[32] Yet, the influence of the seasonal exposure cadence on cardiopulmonary endpoints warrants further investigation, e.g., by replicating the alternation between fire and off-seasons.

4.4. Physical and chemical characteristics of DFS

Alongside breathing patterns, particle size and shape influence location and breadth of deposition within the respiratory tract.[35] While our equipment only allows for measurement of PM size by count (Fig. 2, D), we calculated a mass median aerodynamic diameter of 166 nm for smoldering DFS particulates with assumed 1.18 g/mL density.[56] This estimate agrees with other findings for lab-scale WFS[18,19,92,26] and approaches the lower end of the 0.2–15 μm range obtained from field measurements,[93,94,95,96,97] where $PM_{2.5}$ accounts for the majority of the mass.[25] Note, particles in the fine and ultrafine size range can penetrate deep into the lungs,[35] from where they may either orchestrate the release of mediators of inter-tissue communication[98] or translocate into systemic circulation.[99] Morphological analysis via TEM further revealed that particulates in DFS were mostly circular (Fig. 2, F) and formed agglomerates with an assorted number of primary units (Fig. 2, E). Our findings align with previous evidence showing that smoke particles generated from the combustion of biofuels tend to aggregate,[100,101,102] though the extent to which this occurs may depend on the combustion apparatus.[69]

In addition to the physical characteristics of the PM, the chemical composition of the gaseous and particulate fractions is regarded as a crucial modulator of the biological response to lab-scale WFS inhalation.[23,19,103,104] Amongst the gaseous species in smoldering DFS, the recognized sensory irritants acrolein, formaldehyde, and hydrogen cyanide reached concentrations (Table S3, Supplementary Material) known to induce

respiratory depression in rodents,[105,106,107] consonant with the decreased *RR* of mice exposed to DFS (Table 3). Notably, acrolein and formaldehyde levels in DFS approached or exceeded recommended occupational exposure limits.[5,26,108] Repeated inhalation of these irritants may have further contributed to the long-lasting shifts in cardiopulmonary structure and function of mice exposed to DFS (Figs. 3 and 4), as suggested by previous studies.[109,110,111,112] Prolonged inhalation of benzoic acid at concentrations below those in DFS particulates (Table S2, Supplementary Material) has also been linked to adverse remodeling of the rat lungs.[113] Finally, the particulate fraction of DFS contained chemicals belonging to the class of polycyclic aromatic hydrocarbons (Table S2, Supplementary Material) that were reported to elicit irritant responses in zebrafish, and thus may impose a similar effect on the respiratory tract mucosa in mammals.[103] Notwithstanding this initial chemical analysis, future work should characterize the content of inorganic elements and ionic components, which were related to the induction of toxicity in mice following oropharyngeal aspiration of lab-scale WFS particulates.[104]

4.5. Limitations

Our work relies on the assumption that respiratory and cardiovascular responses to inhaled WFS may depend on the PM cumulatively deposited in the lungs (per unit of surface area) over a set period of time,[114] rather than the PM dose following each exposure instance. While this approach facilitated a preclinical exposure paradigm for predicting the occupational cardiopulmonary risk in mid-career WLFFs, it also constrained the PM concentration delivered to the mice at levels ~40x larger than field measurements.[25] Exposure to smoke at high PM concentrations may have elicited unique biological responses that do not pertain to lower PM levels. Supporting this notion, Martin et al. showed that changes in cardiovascular function, baroreflex sensitivity, and inflammatory response following acute exposure of rats to smoldering peat smoke were concentration dependent.[20] The stunted growth of mice exposed to DFS (Fig. S1, B, Supplementary Material) could indicate overt toxicity, though this effect has been observed across a wide range of cumulative concentrations.[33,87] Furthermore, retention modeling (details in Supplementary Material) confirmed that the deposited particulate volume per mass of mouse lung tissue remained below the 1 μL/g threshold[115] for particle overloading of alveolar macrophages (Fig. S2, Supplementary Material).

The relationships between PM and CO concentrations in the smoke and blood COHb levels as evinced from our data (Fig. 2, A–C) further call into question whether the inhalation of DFS at PM concentrations far above average field measurements may have rendered mice vulnerable to the long-lasting damages of CO intoxication. It is well known that CO inhibits mitochondrial respiration and produces free radicals that contribute to oxidative stress, besides triggering inflammatory effects through platelet activation (see Rose et al.[116] for a review). Since feasibility considerations prompted limiting the daily exposure to 2 hours, we mitigated the risk for CO poisoning by choosing a target PM concentration that maintained COHb levels below the 15% threshold for overt injury.[52] Corresponding CO concentrations in DFS matched the 30–200 ppm range reportedly needed to promote cardiac hypertrophy[117] or ventricular arrhythmia and fibrosis[118] in rodents, yet well surpassed ambient CO levels (<9 ppm) with positive association to elderly hospital admissions for

congestive heart failure.[119,120,121] Measured CO levels also exceeded the 50 ppm 8-hour standard permissible limit enforced by the Occupational Safety and Health Administration (OSHA).[122] Nevertheless, recent data indicate that WLFFs may experience sustained exposure to CO concentrations >100 ppm, depending on the job task.[123] Therefore, while acknowledging that inhalation of CO at high levels may have contributed, at least in part, to the cardiopulmonary decline of exposed mice, we speculate that the relative content of CO in DFS may still be relevant for the WLFF population. Regardless, PM/CO concentration-dependent changes in cardiopulmonary structure and function following long-term WFS exposure demand further evaluation.

5. CONCLUSIONS

To supplement limited epidemiological evidence on the health hazards of wildland firefighting, we evaluated the cardiopulmonary burden in mice exposed to smoldering DFS for a cumulative amount of hours equivalent to a mid-length WLFF career. Smoke inhalation altered breathing patterns in mice, with periods of expiratory braking contributing to a significant reduction in respiratory rate and minute volume. Prolonged exposure to DFS promoted the structural stiffening of the aorta and reduced the ejection fraction of the left ventricle. Compared to air controls, mice exposed to DFS exhibited larger respiratory system resistance at high frequency and increased Newtonian airway resistance due to airway epithelial thickening, with no change in parenchyma tissue properties despite notable septa thickening. These early signs of cardiopulmonary dysfunction in mice exposed to DFS warrant further investigation of the underlying cellular and molecular mechanisms. Future studies should also explore the effect of dosage and exposure frequency on the occupational burden of cardiovascular and respiratory disease due to WFS exposure. Elucidating these aspects is essential for engineering effective personal protective equipment and reducing the adverse health outcomes of wildland firefighting.

Supplementary Material

Refer to Web version on PubMed Central for supplementary material.

ACKNOWLEDGMENTS

We thank Dr. Sara McAllister and Ms. Chelsea Phillips from the United States Department of Agriculture for providing the Douglas fir samples. We acknowledge Dr. Aloisia Schmid from the Boston Electron Microscopy Center at Northeastern University for facilitating TEM analysis of WFS particulates. We express our gratitude to Mr. Nathan Li from the Animal Histology Core at Tufts University for performing embedding, sectioning, and staining of cardiopulmonary tissues. We thank the Center for Translational NeuroImaging (CTNI) at Northeastern University for providing access to the MRI scanner.

FUNDING

This work was supported by DHS/FEMA – EMW-2017-FP-00446 and NIH/NIEHS – R01E5033792 to JMO, CB, and MJG.

NOMENCLATURE

A_p	Particulate area

$\bar{C}$	Average particle matter mass concentration
$\mathscr{D}$	Aortic distensibility
d	Aorta luminal diameter
dep_f	Deposited mass fraction
f_s^j	Duration of a shift segment *j* expressed as a fraction of the average shift duration
H	Coefficient of tissue elastance
G	Coefficient of tissue resistance
L_m	Mean linear intercept
$\dot{m}_{dep}$	Mass deposited per hour of exposure
MV	Minute volume
P	Aorta luminal pressure
P_p	Particulate perimeter
P_{peep}	Positive end expiratory pressure
RR	Respiratory rate
R_N	Airway Newtonian resistance
R_{rs}	Respiratory system resistance
SA	Lung surface area
TV	Tidal volume
t_E	Expiration time
t_I	Inspiration time
t_H	Breath hold time
t_h	Total number of exposure hours
X_{rs}	Respiratory system reactance
Z	Lung impedance
η	Lung tissue hysteresivity
ρ_p	Particulate density
ϕ_{circ}	Particulate circularity
CO	Carbon monoxide

DF	Douglas fir
DFS	Douglas fir smoke
EDV	End-diastolic volume
EF%	Ejection fraction
FRC	Functional residual capacity
FTIR	Fourier-transform infrared
GC-MS	Gas chromatography-mass spectrometry
LRT	Lower respiratory tract
MR	Magnetic resonance
PM	Particulate matter
SV	Stroke volume
TGA	Thermo-gravimetric analyzer
URT	Upper respiratory tract
VOCs	Volatile organic compounds
WFS	Wildland fire smoke
WLFF	Wildland firefighters

References

[1]. Westerling AL, Hidalgo HG, Cayan DR, Swetnam TW, Warming and earlier spring increase western US forest wildfire activity, Science 313 (5789) (2006) 940–943. doi:10.1126/science.1128834. [PubMed: 16825536]

[2]. Caton SE, Hakes RS, Gorham DJ, Zhou A, Gollner MJ, Review of pathways for building fire spread in the wildland urban interface part I: exposure conditions, Fire technology 53 (2) (2017) 429–473. doi:10.1007/s10694-016-0601-7.

[3]. Intergovernmental Panel On Climate Change, Climate change: Impact, adaptation, vulnerability, Available at https://www.ipcc.ch/report/ar5/wg2/ [Online; accessed 12-Nov-2021] (2014).

[4]. Rice MB, Henderson SB, Lambert AA, Cromar KR, Hall JA, Cascio WE, Smith PG, Marsh BJ, Coefield S, Balmes JR, et al. , Respiratory impacts of wildland fire smoke: Future challenges and policy opportunities. an official american thoracic society workshop report, Annals of the American Thoracic Society 18 (6) (2021) 921–930. doi:10.1513/AnnalsATS.202102-148ST. [PubMed: 33938390]

[5]. US Environmental Protection Agency, Air emissions inventories. criteria pollutants national tier 1 for 1970 – 2020. Available at https://www.epa.gov/air-emissions-inventories [Online; accessed 12-Nov-2021].

[6]. Doubleday A, Schulte J, Sheppard L, Kadlec M, Dhammapala R, Fox J, Isaksen TB, Mortality associated with wildfire smoke exposure in washington state, 2006–2017: a case-crossover study, Environmental health 19 (1) (2020) 1–10. doi:10.1186/s12940-020-0559-2. [PubMed: 31898503]

[7]. Faustini A, Alessandrini ER, Pey J, Perez N, Samoli E, Querol X, Cadum E, Perrino C, Ostro B, Ranzi A, et al. , Short-term effects of particulate matter on mortality during forest fires in

southern europe: results of the med-particles project, Occupational and environmental medicine 72 (5) (2015) 323–329. doi:10.1136/oemed-2014-102459. [PubMed: 25691696]

[8]. Johnston F, Hanigan I, Henderson S, Morgan G, Bowman D, Extreme air pollution events from bushfires and dust storms and their association with mortality in Sydney, Australia 1994–2007, Environmental research 111 (6) (2011) 811–816. doi:10.1016/j.envres.2011.05.007. [PubMed: 21601845]

[9]. Morgan G, Sheppeard V, Khalaj B, Ayyar A, Lincoln D, Jalaludin B, Beard J, Corbett S, Lumley T, Effects of bushfire smoke on daily mortality and hospital admissions in Sydney, Australia, Epidemiology (2010) 47–55. doi:10.1097/EDE.0b013e3181c15d5a. [PubMed: 19907335]

[10]. Yao J, Brauer M, Wei J, McGrail KM, Johnston FH, Henderson SB, Sub-daily exposure to fine particulate matter and ambulance dispatches during wildfire seasons: a case-crossover study in British Columbia, Canada, Environmental health perspectives 128 (6) (2020) 067006. doi:10.1289/EHP5792. [PubMed: 32579089]

[11]. Dennekamp M, Straney LD, Erbas B, Abramson MJ, Keywood M, Smith K, Sim MR, Glass DC, Del Monaco A, Haikerwal A, et al. , Forest fire smoke exposures and out-of-hospital cardiac arrests in Melbourne, Australia: a case-crossover study, Environmental health perspectives 123 (10) (2015) 959–964. doi:10.1289/ehp.1408436. [PubMed: 25794411]

[12]. Wettstein ZS, Hoshiko S, Fahimi J, Harrison RJ, Cascio WE, Rappold AG, Cardiovascular and cerebrovascular emergency department visits associated with wildfire smoke exposure in California in 2015, Journal of the American Heart Association 7 (8) (2018) e007492. doi:10.1161/JAHA.117.007492. [PubMed: 29643111]

[13]. Tinling MA, West JJ, Cascio WE, Kilaru V, Rappold AG, Repeating cardiopulmonary health effects in rural North Carolina population during a second large peat wildfire, Environmental Health 15 (1) (2016) 1–12. doi:10.1186/s12940-016-0093-4. [PubMed: 26739281]

[14]. Rappold AG, Stone SL, Cascio WE, Neas LM, Kilaru VJ, Carraway MS, Szykman JJ, Ising A, Cleve WE, Meredith JT, et al. , Peat bog wildfire smoke exposure in rural North Carolina is associated with cardiopulmonary emergency department visits assessed through syndromic surveillance, Environmental health perspectives 119 (10) (2011) 1415–1420. doi:10.1289/ehp.1003206. [PubMed: 21705297]

[15]. Stowell JD, Geng G, Saikawa E, Chang HH, Fu J, Yang C-E, Zhu Q, Liu Y, Strickland MJ, Associations of wildfire smoke PM 2.5 exposure with cardiorespiratory events in Colorado 2011–2014, Environment international 133 (2019) 105151. doi:10.1016/j.envint.2019.105151. [PubMed: 31520956]

[16]. Liu JC, Wilson A, Mickley LJ, Dominici F, Ebisu K, Wang Y, Sulprizio MP, Peng RD, Yue X, Son J-Y, et al. , Wildfire-specific fine particulate matter and risk of hospital admissions in urban and rural counties, Epidemiology (Cambridge, Mass.) 28 (1) (2017) 77. doi:10.1097/EDE.0000000000000556. [PubMed: 27648592]

[17]. Delfino RJ, Brummel S, Wu J, Stern H, Ostro B, Lipsett M, Winer A, Street DH, Zhang L, Tjoa T, et al. , The relationship of respiratory and cardiovascular hospital admissions to the southern California wildfires of 2003, Occupational and environmental medicine 66 (3) (2009) 189–197. doi:10.1136/oem.2008.041376. [PubMed: 19017694]

[18]. Hargrove MM, Kim YH, King C, Wood CE, Gilmour MI, Dye JA, Gavett SH, Smoldering and flaming biomass wood smoke inhibit respiratory responses in mice, Inhalation toxicology 31 (6) (2019) 236–247. doi:10.1080/08958378.2019.1654046. [PubMed: 31431109]

[19]. Kim YH, King C, Krantz T, Hargrove MM, George IJ, McGee J, Copeland L, Hays MD, Landis MS, Higuchi M, et al. , The role of fuel type and combustion phase on the toxicity of biomass smoke following inhalation exposure in mice, Archives of toxicology 93 (6) (2019) 1501–1513. doi:10.1007/s00204-019-02450-5. [PubMed: 31006059]

[20]. Martin BL, Thompson LC, Kim YH, King C, Snow S, Schladweiler M, Haykal-Coates N, George I, Gilmour MI, Kodavanti UP, et al. , Peat smoke inhalation alters blood pressure, baroreflex sensitivity, and cardiac arrhythmia risk in rats, Journal of Toxicology and Environmental Health, Part A 83 (23–24) (2020) 748–763. doi:10.1080/15287394.2020.1826375.

[21]. Martin BL, Thompson LC, Kim YH, Snow SJ, Schladweiler MC, Phillips P, Harmon M, King C, Richards J, George I, et al. , A single exposure to eucalyptus smoke sensitizes rats to the

postprandial cardiovascular effects of a high carbohydrate oral load, Inhalation Toxicology 32 (8) (2020) 342–353. doi:10.1080/08958378.2020.1809572. [PubMed: 32838590]

[22]. Migliaccio CT, Kobos E, King QO, Porter V, Jessop F, Ward T, Adverse effects of wood smoke PM 2.5 exposure on macrophage functions, Inhalation toxicology 25 (2) (2013) 67–76. doi:10.3109/08958378.2012.756086. [PubMed: 23363038]

[23]. Kim YH, Warren SH, Krantz QT, King C, Jaskot R, Preston WT, George BJ, Hays MD, Landis MS, Higuchi M, et al. , Mutagenicity and lung toxicity of smoldering vs. flaming emissions from various biomass fuels: implications for health effects from wildland fires, Environmental health perspectives 126 (1) (2018) 017011. doi:10.1289/EHP2200. [PubMed: 29373863]

[24]. Cuddy JS, Sol JA, Hailes WS, Ruby BC, Work patterns dictate energy demands and thermal strain during wildland firefighting, Wilderness & environmental medicine 26 (2) (2015) 221–226. doi:10.1016/j.wem.2014.12.010. [PubMed: 25772825]

[25]. Navarro KM, Kleinman MT, Mackay CE, Reinhardt TE, Balmes JR, Broyles GA, Ottmar RD, Naher LP, Domitrovich JW, Wildland firefighter smoke exposure and risk of lung cancer and cardiovascular disease mortality, Environmental research 173 (2019) 462–468. doi:10.1016/j.envres.2019.03.060. [PubMed: 30981117]

[26]. Adetona O, Reinhardt TE, Domitrovich J, Broyles G, Adetona AM, Kleinman MT, Ottmar RD, Naeher LP, Review of the health effects of wildland fire smoke on wildland firefighters and the public, Inhalation toxicology 28 (3) (2016) 95–139. doi:10.3109/08958378.2016.1145771. [PubMed: 26915822]

[27]. Naeher LP, Brauer M, Lipsett M, Zelikoff JT, Simpson CD, Koenig JQ, Smith KR, Woodsmoke health effects: a review, Inhalation toxicology 19 (1) (2007) 67–106. doi:10.1080/08958370600985875.

[28]. Coker RH, Murphy CJ, Johannsen M, Galvin G, Ruby BC, Wildland firefighting: adverse influence on indices of metabolic and cardiovascular health, Journal of occupational and environmental medicine 61 (3) (2019) e91. doi:10.1097/JOM.0000000000001535. [PubMed: 30640843]

[29]. Semmens EO, Domitrovich J, Conway K, Noonan CW, A cross-sectional survey of occupational history as a wildland firefighter and health, American journal of industrial medicine 59 (4) (2016) 330–335. doi:10.1002/ajim.22566. [PubMed: 26792645]

[30]. Tesfaigzi Y, Singh SP, Foster JE, Kubatko J, Barr EB, Fine PM, McDonald JD, Hahn FF, Mauderly JL, Health effects of subchronic exposure to low levels of wood smoke in rats, Toxicological Sciences 65 (1) (2002) 115–125. doi:10.1093/toxsci/65.1.115. [PubMed: 11752691]

[31]. Seagrave J, McDonald JD, Reed MD, Seilkop SK, Mauderly JL, Responses to subchronic inhalation of low concentrations of diesel exhaust and hardwood smoke measured in rat bronchoalveolar lavage fluid, Inhalation toxicology 17 (12) (2005) 657–670. doi:10.1080/08958370500189529. [PubMed: 16087572]

[32]. Reed M, Campen M, Gigliotti A, Harrod K, McDonald J, Seagrave J, Mauderly J, Seilkop S, Health effects of subchronic exposure to environmental levels of hardwood smoke, Inhalation toxicology 18 (8) (2006) 523–539. doi:10.1080/08958370600685707. [PubMed: 16717024]

[33]. He F, Liao B, Pu J, Li C, Zheng M, Huang L, Zhou Y, Zhao D, Li B, Ran P, Exposure to ambient particulate matter induced copd in a rat model and a description of the underlying mechanism, Scientific reports 7 (1) (2017) 1–15. doi:10.1038/srep45666. [PubMed: 28127051]

[34]. Anjilvel S, Asgharian B, A multiple-path model of particle deposition in the rat lung, Fundamental and Applied Toxicology 28 (1) (1995) 41–50. doi:10.1006/faat.1995.1144. [PubMed: 8566482]

[35]. Asgharian B, Price O, Oldham M, Chen L-C, Saunders E, Gordon T, Mikheev VB, Minard KR, Teeguarden JG, Computational modeling of nanoscale and microscale particle deposition, retention and dosimetry in the mouse respiratory tract, Inhalation toxicology 26 (14) (2014) 829–842. doi:10.3109/08958378.2014.935535. [PubMed: 25373829]

[36]. Miller FJ, Asgharian B, Schroeter JD, Price O, Improvements and additions to the multiple path particle dosimetry model, Journal of Aerosol Science 99 (2016) 14–26. doi:10.1016/j.jaerosci.2016.01.018.

[37]. Einbrodt H, Hupfeld J, Prager F, Sand H, The suitability of the DIN 53436 test apparatus for the simulation of a fire risk situation with flaming combustion, Journal of fire sciences 2 (6) (1984) 427–438. doi:10.1177/073490418400200603.

[38]. Prager F, Assessment of fire model DIN 53436, Journal of fire sciences 6 (1) (1988) 3–24. doi:10.1177/073490418800600101.

[39]. Garg P, Roche T, Eden M, Matz J, Oakes JM, Bellini C, Gollner MJ, Effect of moisture content and fuel type on emissions from vegetation using a steady state combustion apparatus, International Journal of Wildland Fire 31 (1) (2021) 14–23. doi:10.1071/WF20118.

[40]. Farra YM, Eden MJ, Coleman JR, Kulkarni P, Ferris CF, Oakes JM, Bellini C, Acute neuroradiological, behavioral, and physiological effects of nose-only exposure to vaporized cannabis in C57bl/6 mice, Inhalation toxicology 32 (5) (2020) 200–217. doi:10.1080/08958378.2020.1767237. [PubMed: 32475185]

[41]. Eden MJ, Farra YM, Matz J, Bellini C, Oakes JM, Pharmacological and physiological response in apoe−/− mice exposed to cigarette smoke or e-cigarette aerosols, Inhalation Toxicology (2022) 1–15 doi:10.1080/08958378.2022.2086948.

[42]. Rueden CT, Schindelin J, Hiner MC, DeZonia BE, Walter AE, Arena ET, Eliceiri KW, Imagej2: Imagej for the next generation of scientific image data, BMC bioinformatics 18 (1) (2017) 1–26. doi:10.1186/s12859-017-1934-z. [PubMed: 28049414]

[43]. McGuinn LA, Coull BA, Kloog I, Just AC, Tamayo-Ortiz M, Osorio-Yáñez C, Baccarelli AA, Wright RJ, Téllez-Rojo MM, Wright RO, Fine particulate matter exposure and lipid levels among children in mexico city, Environmental Epidemiology 4 (2) (2020). doi:10.1097/EE9.0000000000000088.

[44]. Mao S, Chen G, Liu F, Li N, Wang C, Liu Y, Liu S, Lu Y, Xiang H, Guo Y, et al. , Long-term effects of ambient air pollutants to blood lipids and dyslipidemias in a chinese rural population, Environmental Pollution 256 (2020) 113403. doi:10.1016/j.envpol.2019.113403. [PubMed: 31711721]

[45]. Knight Lozano CA, Young CG, Burow DL, Hu ZY, Uyeminami D, Pinkerton KE, Ischiropoulos H, Ballinger SW, Cigarette smoke exposure and hypercholesterolemia increase mitochondrial damage in cardiovascular tissues, Circulation 105 (7) (2002) 849–854. doi:10.1161/hc0702.103977. [PubMed: 11854126]

[46]. Lo Sasso G, Schlage WK, Bouè S, Veljkovic E, Peitsch MC, Hoeng J, The apoe−/− mouse model: a suitable model to study cardiovascular and respiratory diseases in the context of cigarette smoke exposure and harm reduction, Journal of translational medicine 14 (1) (2016) 1–16. doi:10.1186/s12967-016-0901-1. [PubMed: 26727970]

[47]. Zhang SH, Reddick RL, Piedrahita JA, Maeda N, Spontaneous hypercholesterolemia and arterial lesions in mice lacking apolipoprotein e, Science 258 (5081) (1992) 468–471. doi:10.1126/science.1411543. [PubMed: 1411543]

[48]. Matz J, Farra YM, Cotto HM, Bellini C, Oakes JM, Respiratory mechanics following chronic cigarette smoke exposure in the apoe−\− mouse model, Biomechanics and Modeling in Mechanobiology (2022) 1–20 doi:10.1007/s10237-022-01644-8.

[49]. Farra YM, Matz J, Ramkhelawon B, Oakes JM, Bellini C, Structural and functional remodeling of the female apoe−/− mouse aorta due to chronic cigarette smoke exposure, American Journal of Physiology-Heart and Circulatory Physiology 320 (6) (2021) H2270–H2282. doi:10.1152/ajpheart.00893.2020. [PubMed: 33834870]

[50]. Oldham MJ, Phalen RF, Robinson RJ, Kleinman MT, Performance of a portable whole-body mouse exposure system, Inhalation toxicology 16 (9) (2004) 657–662. doi:10.1080/08958370490464670. [PubMed: 16036757]

[51]. Wong BA, Inhalation exposure systems: design, methods and operation, Toxicologic Pathology 35 (1) (2007) 3–14. doi:10.1080/01926230601060017. [PubMed: 17325967]

[52]. Wilson MR, O'Dea KP, Dorr AD, Yamamoto H, Goddard ME, Takata M, Efficacy and safety of inhaled carbon monoxide during pulmonary inflammation in mice, PloS one 5 (7) (2010) e11565. doi:10.1371/journal.pone.0011565. [PubMed: 20644637]

[53]. Drorbaug JE, Fenn WO, A barometric method for measuring ventilation in newborn infants, Pediatrics 16 (1) (1955) 81–87. doi:10.1542/peds.16.1.81. [PubMed: 14394741]

[54]. Cruz R, Alves DL, Rumenig E, Gonçalves R, Degaki E, Pasqua L, Koch S, Lima-Silva AE, Koehle MS, Bertuzzi R, Estimation of minute ventilation by heart rate for field exercise studies, Scientific reports 10 (1) (2020) 1–7. doi:10.1038/s41598-020-58253-7. [PubMed: 31913322]

[55]. Oakes JM, Shadden SC, Grandmont C, Vignon-Clementel IE, Aerosol transport throughout inspiration and expiration in the pulmonary airways, International journal for numerical methods in biomedical engineering 33 (9) (2017) e2847. doi:10.1002/cnm.2847.

[56]. Johnson TJ, Olfert JS, Cabot R, Treacy C, Yurteri CU, Dickens C, McAughey J, Symonds JP, Steady-state measurement of the effective particle density of cigarette smoke, Journal of Aerosol Science 75 (2014) 9–16. doi:10.1016/j.jaerosci.2014.04.006.

[57]. Naranjo J, Centeno R, Galiano D, Beaus M, A nomogram for assessment of breathing patterns during treadmill exercise, British journal of sports medicine 39 (2) (2005) 80–83. doi:10.1136/bjsm.2003.009316. [PubMed: 15665202]

[58]. Niinimaa V, Cole P, Shephard R, Oronasal distribution of respiratory airflow, Respiration physiology 43 (1) (1981) 69–75. doi:10.1016/0034-5687(81)90089-x. [PubMed: 7244427]

[59]. Hernandez AB, Kirkness JP, Smith PL, Schneider H, Polotsky M, Richardson RA, Hernandez WC, Schwartz AR, Novel whole body plethysmography system for the continuous characterization of sleep and breathing in a mouse, Journal of applied physiology 112 (4) (2012) 671–680. doi:10.1152/japplphysiol.00818.2011. [PubMed: 22134700]

[60]. Yeh H-C, Schum G, Models of human lung airways and their application to inhaled particle deposition, Bulletin of mathematical biology 42 (3) (1980) 461–480. doi:10.1007/BF02460796. [PubMed: 7378614]

[61]. Adetona O, Dunn K, Hall DB, Achtemeier G, Stock A, Naeher LP, Personal PM 2.5 exposure among wildland firefighters working at prescribed forest burns in southeastern united states, Journal of occupational and environmental hygiene 8 (8) (2011) 503–511. doi:10.1080/15459624.2011.595257. [PubMed: 21762011]

[62]. Baek S, Gleason RL, Rajagopal K, Humphrey J, Theory of small on large: potential utility in computations of fluid–solid interactions in arteries, Computer methods in applied mechanics and engineering 196 (31–32) (2007) 3070–3078. doi:10.1016/j.cma.2006.06.018.

[63]. Heiberg E, Sjögren J, Ugander M, Carlsson M, Engblom H, Arheden H, Design and validation of segment-freely available software for cardiovascular image analysis, BMC medical imaging 10 (1) (2010) 1–13. doi:10.1186/1471-2342-10-1. [PubMed: 20064248]

[64]. Bates JH, Corp: Measurement of lung function in small animals, Journal of Applied Physiology 123 (5) (2017) 1039–1046. doi:10.1152/japplphysiol.00243.2017. [PubMed: 28798197]

[65]. Hantos Z, Daroczy B, Suki B, Nagy S, Fredberg J, Input impedance and peripheral inhomogeneity of dog lungs, Journal of applied physiology 72 (1) (1992) 168–178. doi:10.1152/jappl.1992.72.1.168. [PubMed: 1537711]

[66]. Bates JH, Lung mechanics: an inverse modeling approach, Cambridge University Press, 2009.

[67]. Akagi S, Yokelson RJ, Wiedinmyer C, Alvarado M, Reid J, Karl T, Crounse J, Wennberg P, Emission factors for open and domestic biomass burning for use in atmospheric models, Atmospheric Chemistry and Physics 11 (9) (2011) 4039–4072. doi:10.5194/acp-11-4039-2011.

[68]. Jen CN, Hatch LE, Selimovic V, Yokelson RJ, Weber R, Fernandez AE, Kreisberg NM, Barsanti KC, Goldstein AH, Speciated and total emission factors of particulate organics from burning western us wildland fuels and their dependence on combustion efficiency, Atmospheric Chemistry and Physics 19 (2) (2019) 1013–1026. doi:10.5194/acp-19-1013-2019.

[69]. Just B, Rogak S, Kandlikar M, Characterization of ultrafine particulate matter from traditional and improved biomass cookstoves, Environmental science & technology 47 (7) (2013) 3506–3512. doi:10.1021/es304351p. [PubMed: 23469776]

[70]. O'Rourke MF, Arterial aging: pathophysiological principles, Vascular medicine 12 (4) (2007) 329–341. doi:10.1177/1358863X07083392. [PubMed: 18048471]

[71]. Cascio WE, Wildland fire smoke and human health, Science of the total environment 624 (2018) 586–595. doi:10.1016/j.scitotenv.2017.12.086. [PubMed: 29272827]

[72]. Groot E, Caturay A, Khan Y, Copes R, A systematic review of the health impacts of occupational exposure to wildland fires, International journal of occupational medicine and environmental health 32 (2) (2019) 121–140. doi:10.13075/ijomeh.1896.01326. [PubMed: 30919829]

[73]. Koopmans E, Cornish K, Fyfe TM, Bailey K, Pelletier CA, Health risks and mitigation strategies from occupational exposure to wildland fire: a scoping review, Journal of Occupational Medicine and Toxicology 17 (1) (2022) 1–17. doi:10.1186/s12995-021-00328-w. [PubMed: 34980168]

[74]. Pelletier C, Ross C, Bailey K, Fyfe TM, Cornish K, Koopmans E, Health research priorities for wildland firefighters: a modified delphi study with stakeholder interviews, BMJ open 12 (2) (2022) e051227. doi:10.1136/bmjopen-2021-051227.

[75]. Mitchell GF, Hwang S-J, Vasan RS, Larson MG, Pencina MJ, Hamburg NM, Vita JA, Levy D, Benjamin EJ, Arterial stiffness and cardiovascular events: the framingham heart study,Circulation 121 (4) (2010) 505–511. doi:10.1161/CIRCULATIONAHA.109.886655. [PubMed: 20083680]

[76]. Gaughan DM, Siegel PD, Hughes MD, Chang C-Y, Law BF, Campbell CR, Richards JC, Kales SF, Chertok M, Kobzik L, et al. , Arterial stiffness, oxidative stress, and smoke exposure in wildland firefighters, American journal of industrial medicine 57 (7) (2014a) 748–756. doi:10.1002/ajim.22331. [PubMed: 24909863]

[77]. Martin BL, Thompson LC, Kim Y, Williams W, Snow SJ, Schladweiler MC, Phillips P, King C, Richards J, Haykal-Coates N, et al. , Acute peat smoke inhalation sensitizes rats to the postprandial cardiometabolic effects of a high fat oral load, Science of The Total Environment 643 (2018) 378–391. doi:10.1016/j.scitotenv.2018.06.089. [PubMed: 29940449]

[78]. Betchley C, Koenig JQ, van Belle G, Checkoway H, Reinhardt T, Pulmonary function and respiratory symptoms in forest firefighters, American journal of industrial medicine 31 (5) (1997) 503–509. doi:10.1002/(sici)1097-0274(199705)31:5<503::aid-ajim3>3.0.co;2-u. [PubMed: 9099351]

[79]. Jacquin L, Michelet P, Brocq F-X, Houel J-G, Truchet X, Auffray J-P, Carpentier J-P, Jammes Y, Short-term spirometric changes in wildland firefighters, American journal of industrial medicine 54 (11) (2011) 819–825. doi:10.1002/ajim.21002. [PubMed: 22006591]

[80]. Adetona O, Hall DB, Naeher LP, Lung function changes in wildland firefighters working at prescribed burns, Inhalation toxicology 23 (13) (2011) 835–841. doi:10.3109/08958378.2011.617790. [PubMed: 22035123]

[81]. Gaughan DM, Cox-Ganser JM, Enright PL, Castellan RM, Wagner GR, Hobbs GR, Bledsoe TA, Siegel PD, Kreiss K, Weissman DN, Acute upper and lower respiratory effects in wildland firefighters, Journal of occupational and environmental medicine 50 (9) (2008) 1019–1028. doi:10.1097/JOM.0b013e3181754161. [PubMed: 18784550]

[82]. Liu D, Tager IB, Balmes JR, Harrison RJ, The effect of smoke inhalation on lung function and airway responsiveness in wildland fire fighters, American Review of Respiratory Disease 146 (1992) 1469–1469. doi:10.1164/ajrccm/146.6.1469. [PubMed: 1456562]

[83]. Miranda AI, Martins V, Cascão P, Amorim JH, Valente J, Borrego C, Ferreira AJ, Cordeiro CR, Viegas DX, Ottmar R, Wildland smoke exposure values and exhaled breath indicators in firefighters, Journal of Toxicology and Environmental Health, Part A 75 (13–15) (2012) 831–843. doi:10.1080/15287394.2012.690686.

[84]. Rothman N, Ford DP, Baser ME, Hansen JA, O'Toole T, Tockman MS, Strickland PT, Pulmonary function and respiratory symptoms in wildland firefighters., Journal of occupational medicine.: official publication of the Industrial Medical Association 33 (11) (1991) 1163–1167. doi:10.1097/00043764-199111000-00013. [PubMed: 1765858]

[85]. Leigh R, Ellis R, Wattie J, Southam DS, De Hoogh M, Gauldie J, O'Byrne PM, Inman MD, Dysfunction and remodeling of the mouse airway persist after resolution of acute allergen-induced airway inflammation, American journal of respiratory cell and molecular biology 27 (5) (2002) 526–535. doi:10.1165/rcmb.2002-0048OC. [PubMed: 12397011]

[86]. Massaro D, Massaro GD, Apoetm1unc mice have impaired alveologenesis, low lung function, and rapid loss of lung function, American Journal of Physiology-Lung Cellular and Molecular Physiology 294 (5) (2008) L991–L997. doi:10.1152/ajplung.00013.2008. [PubMed: 18344414]

[87]. Ramos C, Cisneros J, Gonzalez-Avila G, Becerril C, Ruiz V, Montano M, Increase of matrix metalloproteinases in woodsmoke-induced lung emphysema in guinea pigs, Inhalation toxicology 21 (2) (2009) 119–132. doi:10.1080/08958370802419145. [PubMed: 18836920]

[88]. Ramos C, Cañedo-Mondragón R, Becerril C, González-Ávila G, Esquivel AL, Torres-Machorro AL, Montaño M, Short-term exposure to wood smoke increases the expression of pro-

inflammatory cytokines, gelatinases, and timps in guinea pigs, Toxics 9 (9) (2021) 227. doi:10.3390/toxics9090227. [PubMed: 34564378]

[89]. Alarie Y, Sensory irritation by airborne chemicals, CRC critical reviews in toxicology 2 (3) (1973) 299–363. doi:10.3109/10408447309082020. [PubMed: 4131690]

[90]. Vijayaraghavan R, Schaper M, Thompson R, Stock M, Alarie Y, Characteristic modifications of the breathing pattern of mice to evaluate the effects of airborne chemicals on the respiratory tract, Archives of toxicology 67 (7) (1993) 478–490. doi:10.1007/BF01969919. [PubMed: 8239997]

[91]. Booze TF, Reinhardt TE, Quiring SJ, Ottmar RD, A screening-level assessment of the health risks of chronic smoke exposure for wildland firefighters, Journal of occupational and environmental hygiene 1 (5) (2004) 296–305. doi:10.1080/15459620490442500. [PubMed: 15238338]

[92]. Kleeman MJ, Schauer JJ, Cass GR, Size and composition distribution of fine particulate matter emitted from wood burning, meat charbroiling, and cigarettes, Environmental Science & Technology 33 (20) (1999) 3516–3523. doi:10.1021/es981277q.

[93]. McMeeking G, Kreidenweis S, Carrico C, Lee T, Collett J Jr, Malm W, Observations of smokeinfluenced aerosol during the yosemite aerosol characterization study: Size distributions and chemical composition, Journal of Geophysical Research: Atmospheres 110 (D9) (2005) . doi:10.1029/2004JD005389.

[94]. Gaughan DM, Piacitelli CA, Chen BT, Law BF, Virji MA, Edwards NT, Enright PL, Schwegler-Berry DE, Leonard SS, Wagner GR, et al. , Exposures and cross-shift lung functiondeclines in wildland firefighters, Journal of occupational and environmental hygiene 11 (9) (2014b) 591–603. doi:10.1080/15459624.2014.895372. [PubMed: 24568319]

[95]. Kleinman LI, Sedlacek III AJ, Adachi K, Buseck PR, Collier S, Dubey MK, Hodshire AL, Lewis E, Onasch TB, Pierce JR, et al. , Rapid evolution of aerosol particles and their optical properties downwind of wildfires in the western US, Atmospheric Chemistry and Physics 20 (21) (2020) 13319–13341. doi:10.5194/acp-20-13319-2020.

[96]. Leonard SS, Castranova V, Chen BT, Schwegler-Berry D, Hoover M, Piacitelli C, Gaughan DM, Particle size-dependent radical generation from wildland fire smoke, Toxicology 236 (1–2) (2007) 103–113. doi:10.1016/j.tox.2007.04.008. [PubMed: 17482744]

[97]. Keywood MD, Ayers GP, Gras JL, Gillett RW, Cohen DD, Size distribution and sources of aerosol in Launceston, Australia, during winter 1997, Journal of the Air & Waste Management Association 50 (3) (2000) 418–427. doi:10.1080/10473289.2000.10464022. [PubMed: 10734713]

[98]. Carberry CK, Koval LE, Payton A, Hartwell H, Kim YH, Smith GJ, Reif DM, Jaspers I, Gilmour MI, Rager JE, Wildfires and extracellular vesicles: Exosomal micrornas as mediators of cross-tissue cardiopulmonary responses to biomass smoke, Environment International (2022) 107419 doi:10.1016/j.envint.2022.107419. [PubMed: 35863239]

[99]. Kolanjiyil AV, Kleinstreuer C, Nanoparticle mass transfer from lung airways to systemic regions—part II: Multi-compartmental modeling, Journal of biomechanical engineering 135 (12). doi:10.1115/1.4025333.

[100]. Patiño D, Pérez-Orozco R, Porteiro J, Lapuerta M, Characterization of biomass PM emissions using thermophoretic sampling: Composition and morphological description of the carbonaceous residues, Journal of Aerosol Science 127 (2019) 49–62. doi:10.1016/j.jaerosci.2018.10.005.

[101]. Oo HM, Karin P, Chollacoop N, Hanamura K, Physicochemical characterization of forest and sugarcane leaf combustion's particulate matters using electron microscopy, eds, xrd and tga, Journal of Environmental Sciences 99 (2021) 296–310. doi:10.1016/j.jes.2020.06.036.

[102]. Longhin E, Gualtieri M, Capasso L, Bengalli R, Mollerup S, Holme JA, Øvrevik J, Casadei S, Di Benedetto C, Parenti P, et al. , Physico-chemical properties and biological effects of diesel and biomass particles, Environmental Pollution 215 (2016) 366–375. doi:10.1016/j.envpol.2016.05.015. [PubMed: 27194366]

[103]. Martin WK, Padilla S, Kim Y, Hunter D, Hays M, DeMarini D, Hazari M, Gilmour M, Farraj A, Zebrafish irritant responses to wildland fire-related biomass smoke are influenced by fuel type, combustion phase, and byproduct chemistry, Journal of Toxicology and Environmental Health, Part A 84 (16) (2021) 674–688. doi:10.1080/15287394.2021.1925608.

[104]. Rager JE, Clark J, Eaves LA, Avula V, Niehoff NM, Kim YH, Jaspers I, Gilmour MI, Mixtures modeling identifies chemical inducers versus repressors of toxicity associated with wildfire smoke, Science of The Total Environment 775 (2021) 145759. doi:10.1016/j.scitotenv.2021.145759. [PubMed: 33611182]

[105]. Kane LE, Alarie Y, interactions of sulfur dioxide and acrolein as sensory irritants, Toxicology and Applied Pharmacology 48 (2) (1979) 305–315. doi:10.1016/0041-008X(79)90037-1. [PubMed: 473180]

[106]. Chang J, Steinhagen W, Barrow C, Effect of single or repeated formaldehyde exposure on minute volume of b6c3f1 mice and f-344 rats, Toxicology and Applied Pharmacology 61 (3) (1981) 451–459. doi:10.1016/0041-008X(81)90368-9. [PubMed: 7330883]

[107]. Matijak Schaper M, Alarie Y, Toxicity of carbon monoxide, hydrogen cyanide and low oxygen, J. Combust. Toxicol.;(United States) 9, https://www.osti.gov/biblio/6373463.

[108]. Reinhardt TE, Smoke exposure at western wildfires, Tech. rep (2000).

[109]. Costa DL, Kutzman RS, Lehmann JR, Drew RT, Altered lung function and structure in the rat after subchronic exposure to acrolein, American Review of Respiratory Disease 133 (2) (1986) 286–291. doi:10.1164/arrd.1986.133.2.286. [PubMed: 3946923]

[110]. Conklin DJ, Malovichko MV, Zeller I, Das TP, Krivokhizhina TV, Lynch BH, Lorkiewicz P, Agarwal A, Wickramasinghe N, Haberzettl P, et al. , Biomarkers of chronic acrolein inhalation exposure in mice: implications for tobacco product-induced toxicity, Toxicological Sciences 158 (2) (2017) 263–274. doi:10.1093/toxsci/kfx095. [PubMed: 28482051]

[111]. Zhang X, Zhao Y, Song J, Yang X, Zhang J, Zhang Y, Li R, Differential health effects of constant versus intermittent exposure to formaldehyde in mice: implications for building ventilation strategies, Environmental science & technology 52 (3) (2018) 1551–1560. doi:10.1021/acs.est.7b05015. [PubMed: 29293324]

[112]. Li L, Hua L, He Y, Bao Y, Differential effects of formaldehyde exposure on airway inflammation and bronchial hyperresponsiveness in balb/c and c57bl/6 mice, PLoS One 12 (6) (2017) e0179231. doi:10.1371/journal.pone.0179231. [PubMed: 28591193]

[113]. US Environmental Protection Agency, provisional peer reviewed toxicity values for benzoic acid Available at https://cfpub.epa.gov/ncea/pprtv/documents/BenzoicAcid.pdf [Online; accessed 22-Aug-2022].

[114]. Thomas DC, Invited commentary: is it time to retire the “pack-years” variable? maybe not!, American journal of epidemiology 179 (3) (2014) 299–302. doi:10.1093/aje/kwt274. [PubMed: 24355333]

[115]. Oberdorster G, Lung particle overload: implications for occupational exposures to particles, Regulatory Toxicology and Pharmacology 21 (1) (1995) 123–135. doi:10.1006/rtph.1995.1017. [PubMed: 7784625]

[116]. Rose JJ, Wang L, Xu Q, McTiernan CF, Shiva S, Tejero J, Gladwin MT, Carbon monoxide poisoning: pathogenesis, management, and future directions of therapy, American journal of respiratory and critical care medicine 195 (5) (2017) 596–606. doi:10.1164/rccm.201606-1275CI. [PubMed: 27753502]

[117]. Sørhaug S, Steinshamn S, Nilsen OG, Waldum HL, Chronic inhalation of carbon monoxide: effects on the respiratory and cardiovascular system at doses corresponding to tobacco smoking, Toxicology 228 (2–3) (2006) 280–290. doi:10.1016/j.tox.2006.09.008. [PubMed: 17056171]

[118]. Andre L, Boissière J, Reboul C, Perrier R, Zalvidea S, Meyer G, Thireau J, Tanguy S, Bideaux P, Hayot M, et al. , Carbon monoxide pollution promotes cardiac remodeling and ventricular arrhythmia in healthy rats, American journal of respiratory and critical care medicine 181 (6) (2010) 587–595. doi:10.1164/rccm.200905-0794OC. [PubMed: 20019346]

[119]. Townsend C, Maynard R, Effects on health of prolonged exposure to low concentrations of carbon monoxide, Occupational and Environmental Medicine 59 (10) (2002) 708–711. doi:10.1136/oem.59.10.708. [PubMed: 12356933]

[120]. Morris RD, Naumova EN, Munasinghe RL, Ambient air pollution and hospitalization for congestive heart failure among elderly people in seven large us cities., American journal of public health 85 (10) (1995) 1361–1365. doi:10.2105/ajph.85.10.1361. [PubMed: 7573618]

[121]. Burnett RT, Dales RE, Brook JR, Raizenne ME, Krewski D, Association between ambient carbon monoxide levels and hospitalizations for congestive heart failure in the elderly in 10 canadian cities, Epidemiology (1997) 162–167 doi:10.1097/00001648-199703000-00007. [PubMed: 9229208]

[122]. Occupational Safety, H. Administration, OSHA Occupational Chemical Database: Carbon monoxide, Available at https://www.osha.gov/chemicaldata/462 [Online; accessed 17-Nov-2022].

[123]. Semmens EO, Leary CS, West MR, Noonan CW, Navarro KM, Domitrovich JW, Carbon monoxide exposures in wildland firefighters in the united states and targets for exposure reduction, Journal of exposure science & environmental epidemiology 31 (5) (2021) 923–929. doi:10.1038/s41370-021-00371-z. [PubMed: 34285366]

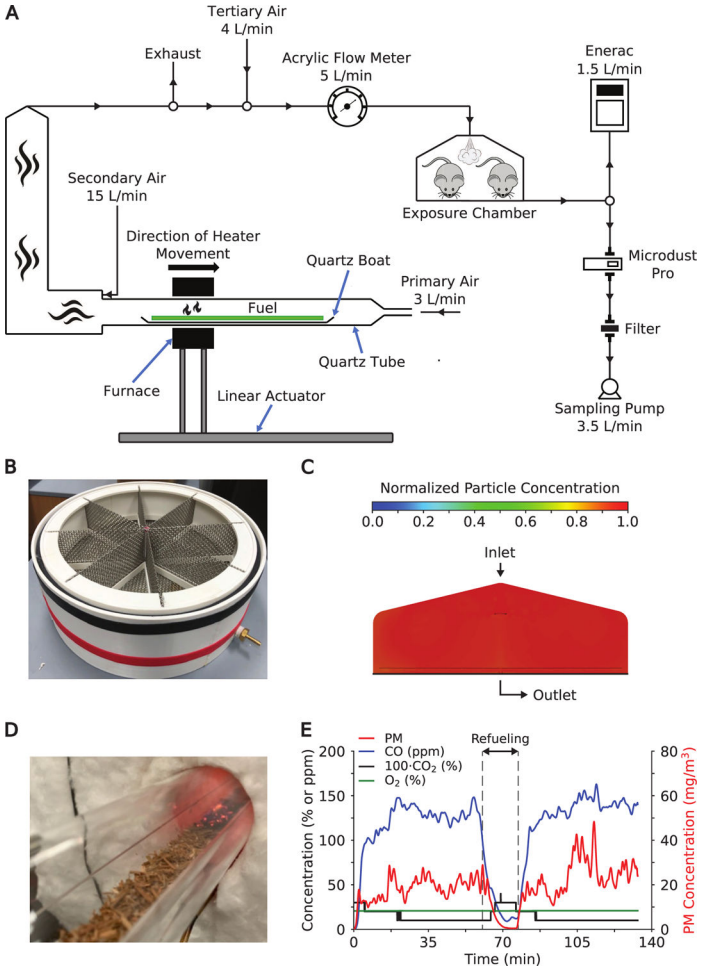

Figure 1:

Custom apparatus for consistent generation and homogeneous delivery of smoldering DFS to a mouse whole-body exposure chamber. A ring furnace produces DFS that is diluted **(A)** and propelled to the exposure chamber **(B)**. The design of the exposure chamber was iteratively refined until physics-based simulations predicted a homogeneous distribution of the smoke within each compartment **(C)**. The ring furnace is mounted onto a linear actuator and generates smoldering combustion as it travels over the dried Douglas fir needles at 450 °C **(D)**. Daily exposure consists of two, 1 hour-long sessions separated by a brief refueling period, after which PM and CO concentrations in DFS quickly stabilize **(E)**.

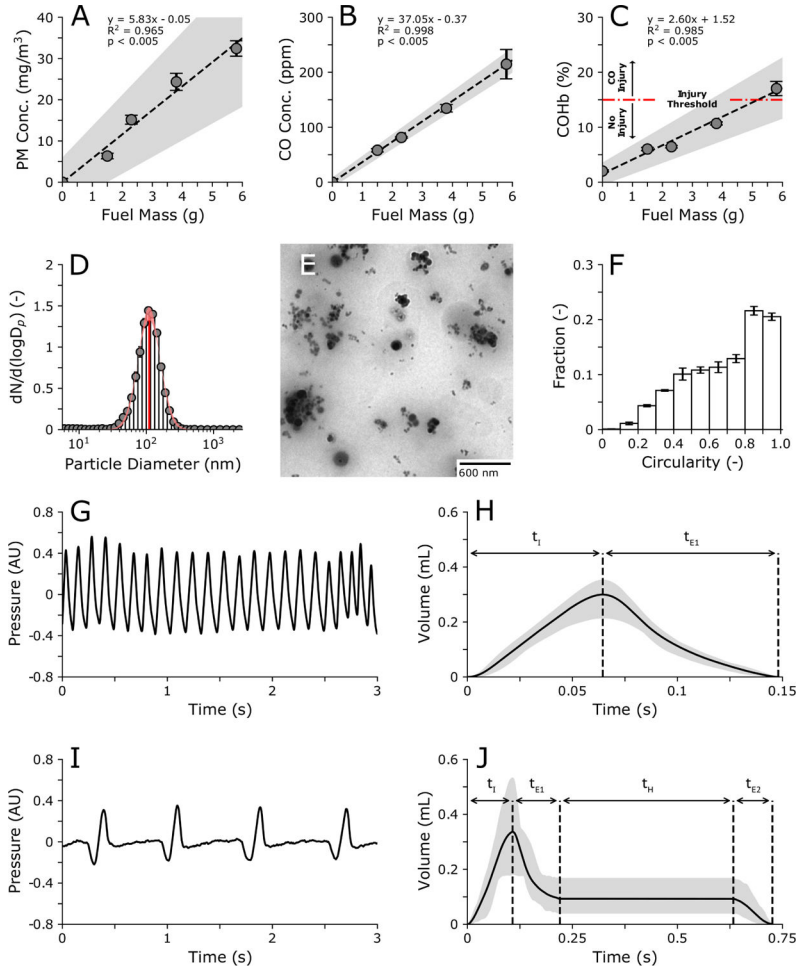

Figure 2:

Mice tolerate inhalation of respirable PM in DFS but consistently exhibit expiratory flow interruption. Concentrations of PM **(A)** and CO **(B)** in DFS and COHb levels in the blood of exposed mice **(C)** increase linearly with the mass of combusted fuel. Aerosol analysis and health assessments presented hereafter leverage a fuel load of 3.75g to maximize emissions without exceeding the threshold for CO-mediated toxicity **(C)**. Under these conditions, the count distribution of particle sizes in DFS is unimodal and follows a lognormal probability function (red shaded area) **(D)**. Processing of TEM images confirms that individual particles and agglomerates in DFS **(E)** are mostly circular in shape **(F)**. Traces of pressure signals in a wholebody plethysmograph reveal expiratory braking in mice exposed to DFS **(I)** and corroborate normal breathing in air controls **(G)**. Note, a rise in pressure (i.e., positive slope) is indicative of inhalation, whereas a drop in pressure (i.e., negative slope) corresponds to exhalation. As a result, the representative volume curve under DFS exposure conditions comprises inspiration, primary expiration, breath hold, and secondary expiration phases **(J)**, while inspiration and expiration alone appear in the case of air exposure **(H)**. Black solid lines delineate average values while grey shaded areas reflect 95% confidence intervals. Note, the scale on the x-axis for panels **(H)** and **(J)** matches the *RR* of mice exposed to HEPA-filtered air or DFS, respectively (Table 3).

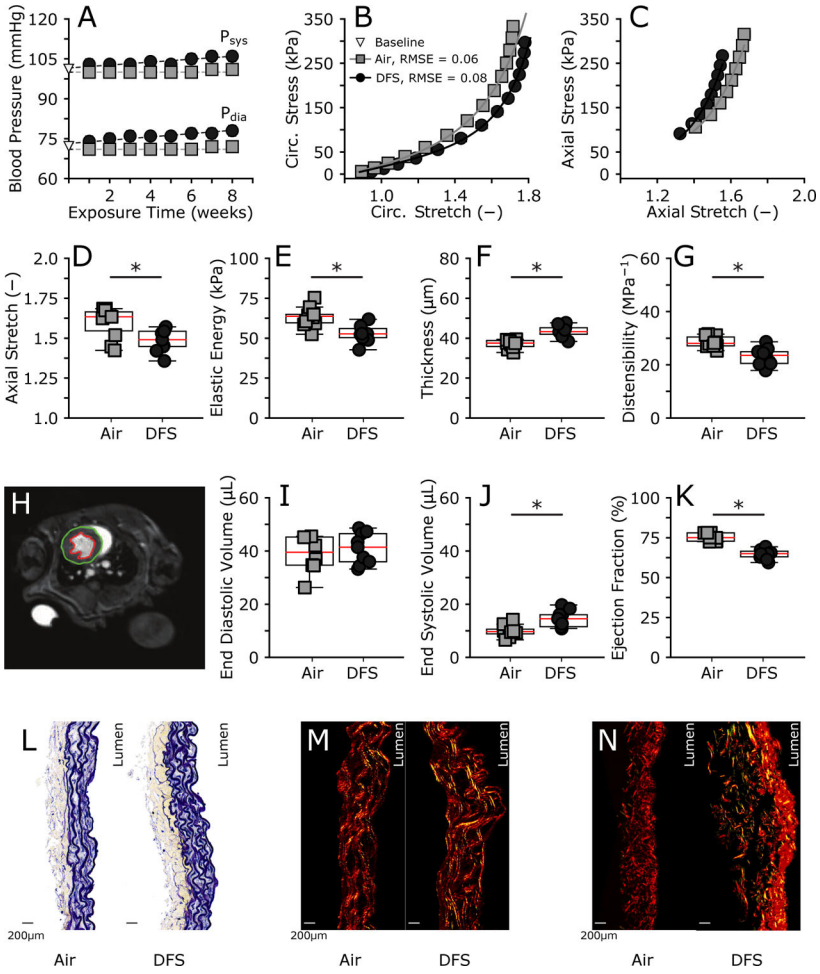

Figure 3:

Daily inhalation of DFS over 8 weeks promotes structural stiffening of the abdominal aorta and triggers cardiovascular dysfunction. Peripheral blood pressure increases linearly over time in mice exposed to DFS but remains at baseline in air controls **(A)**. When subjected to the same stress, tissues from the aorta of DFS-exposed mice experience higher circumferential **(B)** and lower axial **(C)** deformations compared to air controls. Solid line predictions in panels **(B)** and **(C)** are based upon best-fit values for the coefficients of the strain energy potential pertaining to group average data (Equation S.14, Supplementary Material). Fitting of individual data sets facilitated additional calculation of geometrical and mechanical metrics under physiological loads. Amongst those, prolonged inhalation of DFS reduces axial extensibility **(D)** and limits the amount of elastic energy for diastolic blood flow augmentation **(E)**. Wall thickening **(F)** contributes to decreasing the distensibility of the DFS aorta within the range of *in vivo* pressures **(G)**. Consistently, segmentation of left ventricular volumes from cardiac MR images **(H)** reveals increased end-systolic volume **(J)** with preserved end-diastolic volume **(I)**, supporting a significant decline in ejection fraction **(K)**. Movat's pentachrome stained cross-sections confirm thickening of the aortic wall with DFS exposure **(L)**. Picrosirius red stained cross-sections imaged under polarized light further suggest preserved medial collagen **(M)** and adventitial collagen deposition **(N)**

in the DFS group. Statistically significant difference between groups denoted as * overbar for $p<0.05$.

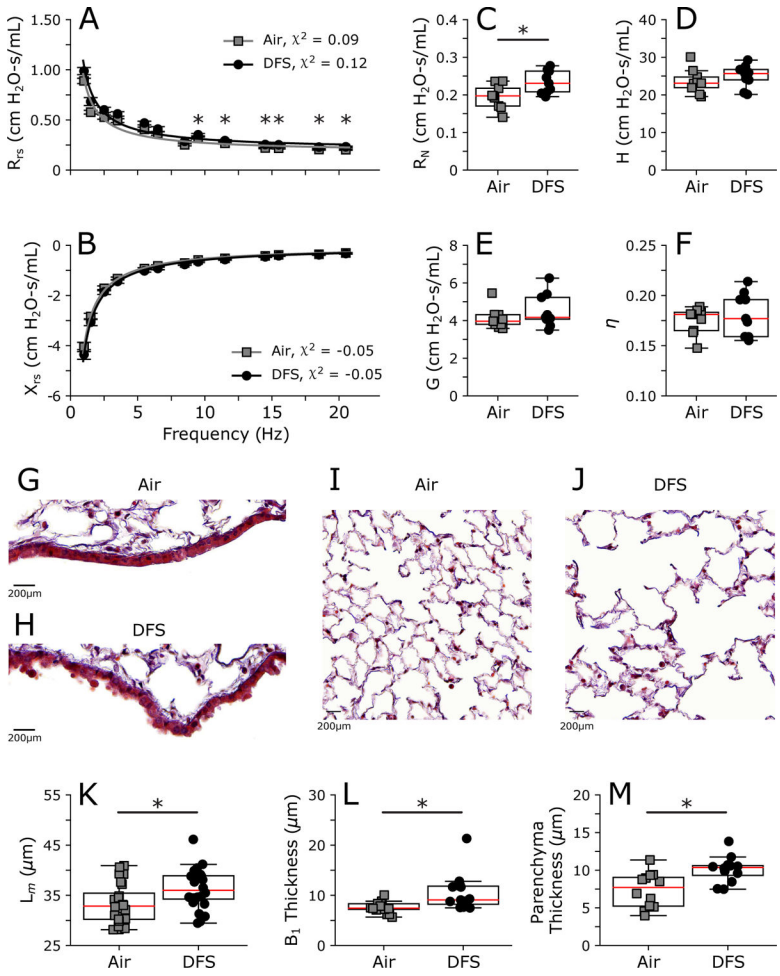

Figure 4:

Remodeling of the airways following 8 weeks of daily DFS inhalation increases the Newtonian resistance. Mice exposed to DFS exhibit larger respiratory system resistance (R_{rs}) than air controls when ventilated at or above 9.5 Hz and 1 cmH_2O P_{peep} **(A)**. No difference in reactance (X_{rs}) emerges between the two groups at any frequency and 1 cmH_2O P_{peep} **(B)**. Solid lines superimposed to real **(A)** and imaginary **(B)** components of impedance rely on best-fit parameters for the constant phase model in Equation 6, as estimated from group average data. Fitting the constant phase model to individual impedance data at 1 cmH_2O P_{peep} further provided within-group variability for parameters R_N, H, and G, alongside the derived metric η. Exposure to DFS augments airway resistance **(C)** but preserves the coefficient of tissue elastance **(D)**, the coefficient of tissue resistance **(E)**, and therefore lung tissue hysteresivity **(F)**. Morphological analysis of Movat's pentachorme stained airway **(G–H)** and parenchyma **(I–J)** tissues reveals airspace enlargement **(K)** as well as thickening of epithelial cell-laden airways **(L)** and alveolar septa **(M)** following DFS exposure. Statistically significant difference between groups denoted as * overbar for $p<0.05$.

Table 1:

WLFFs are expected to experience a weighted average PM mass deposition rate per shift hour ($\dot{m}_{dep}$) of 0.42 mg/hr.

HR^j	f_s^j	MV^j	TV^j	RR^j	dep_f^j	$\dot{m}_{dep}^j$
Beats/min	**-**	**L/min**	**L**	**Breaths/min**	**-**	**mg/hr**
<100	0.37	21.2	1.1	19.1	0.321	0.077
100–120	0.25	32.2	1.4	23.4	0.327	0.081
120–140	0.20	49.0	1.7	29.2	0.338	0.101
140–160	0.12	74.6	2.0	37.1	0.342	0.094
160–180	0.04	113.5	2.4	48.2	0.350	0.049
≥180	0.01	172.8	2.7	63.5	0.349	0.018

A typical shift is partitioned into segments by heart rate (*HR*) and corresponding ventilation parameters (minute volume *MV*; tidal volume *TV*; respiration rate *RR*). Applied weights are relative shift segment lengths expressed as fractions of the entire shift duration (f_s). Deposition fractions (dep_f) as predicted from dosimetry modeling (see Supplementary Material). Index *j* sweeps through the activity levels. Note, all calculations assume constant PM concentration of $\bar{C}$ = 0.51 mg/m^3 throughout the shift.

Table 2:

Exposure parameters that yield equivalent deposited mass per unit of surface area in the LRT of mice and WLFFs.

			WLFF	
PM concentration	$\bar{C}_W$	mg/m^3	0.51	*A*
Deposited PM mass per hour	$\dot{m}_{dep,W}$	mg/hr	0.42	
Cumulative exposure hours	$t_{h,W}$	hrs	3600	
Hours per shift	t_s	hrs	10.3 – 13.6	*A*,*B*
Shifts per year	n_s	days	49 – 98	*A*
Years of service		years	3 – 7	
Lung surface area	SA_W	m^2	67.5	*C*
			Mouse	
PM concentration	$\bar{C}_M$	mg/m^3	22	
Deposited PM mass per hour	$\dot{m}_{dep,M}$	mg/hr	0.0126	
Cumulative exposure hours	$t_{h,M}$	hrs	80	
Exposure hours per day		hrs	2	
Exposure days per week		days	5	
Weeks of exposure		weeks	8	
Lung surface area	SA_M	m^2	0.0454	*D*

*A*Navarro et al. (2019);

*B*Adetona et al. (2011);

*C*Yeh & Schum (1980);

*D*Asgharian et al. (2014).

Note, dosimetry calculations for both species sweep the range of particle sizes in DFS (Fig. 2, D). Also, the fraction of inhaled mass that deposits in LRT of WLFFs varies during a shift depending on MV ($dep_{f,M}$; Table 1), while $dep_{f,M}$ = 0.354 in mice assuming the same MV throughout exposure.

Table 3:

Expiratory braking decreases breathing frequency but preserves tidal volume in mice exposed to WFS, compared with baseline conditions when inhaling air.

	RR	TV	MV	t_I	t_{E_1}	t_H	t_{E_2}
	breaths/min	**mL**	**mL/min**	**ms**	**ms**	**ms**	**ms**
Air (baseline)	404 ± 8	0.30 ± 0.02	122 ± 8	65 ± 3	84 ± 4	-	-
DFS	83 ± 10*	0.34 ± 0.05	27 ± 4*	107 ± 5*	119 ± 21	508 ± 118	99 ± 10

RR: respiratory rate, TV: tidal volume, MV: minute volume, t_I: inspiration time, t_E: expiration time, t_H: hold.

Subscripts 1 and 2 further differentiate between the first and second expiratory periods, if present.

Statistically significant difference between groups denoted as * for $p < 0.05$.